

## The effects of low oxidation-reduction potential on the performance of full-scale hybrid membrane-aerated biofilm reactors

Uri-Carreño, Nerea; Nielsen, Per H.; Gernaey, Krist V.; Wang, Qian; Nielsen, Ulla Gro; Nierychlo, Marta; Hansen, Susan H.; Thomsen, Lisette; Flores-Alsina, Xavier

*Published in:*  
Chemical engineering journal

*DOI (link to publication from Publisher):*  
[10.1016/j.cej.2022.138917](https://doi.org/10.1016/j.cej.2022.138917)

*Creative Commons License*  
CC BY 4.0

*Publication date:*  
2023

*Document Version*  
Publisher's PDF, also known as Version of record

[Link to publication from Aalborg University](#)

*Citation for published version (APA):*  
Uri-Carreño, N., Nielsen, P. H., Gernaey, K. V., Wang, Q., Nielsen, U. G., Nierychlo, M., Hansen, S. H., Thomsen, L., & Flores-Alsina, X. (2023). The effects of low oxidation-reduction potential on the performance of full-scale hybrid membrane-aerated biofilm reactors. *Chemical engineering journal*, 451, Article 138917. <https://doi.org/10.1016/j.cej.2022.138917>

### General rights

Copyright and moral rights for the publications made accessible in the public portal are retained by the authors and/or other copyright owners and it is a condition of accessing publications that users recognise and abide by the legal requirements associated with these rights.

- Users may download and print one copy of any publication from the public portal for the purpose of private study or research.
- You may not further distribute the material or use it for any profit-making activity or commercial gain
- You may freely distribute the URL identifying the publication in the public portal -

### Take down policy

If you believe that this document breaches copyright please contact us at [vbn@aub.aau.dk](mailto:vbn@aub.aau.dk) providing details, and we will remove access to the work immediately and investigate your claim.





# The effects of low oxidation-reduction potential on the performance of full-scale hybrid membrane-aerated biofilm reactors

Nerea Uri-Carreño<sup>a,b,\*</sup>, Per H. Nielsen<sup>a</sup>, Krist V. Gernaey<sup>b</sup>, Qian Wang<sup>c</sup>, Ulla Gro Nielsen<sup>c</sup>, Marta Nierychlo<sup>d</sup>, Susan H. Hansen<sup>d</sup>, Lisette Thomsen<sup>d</sup>, Xavier Flores-Alsina<sup>b</sup>

<sup>a</sup> Vandcenter Syd A/S, Vandværksvej 7, Odense 5000, Denmark

<sup>b</sup> Process and Systems Engineering Center (PROSYS), Department of Chemical and Biochemical Engineering, Technical University of Denmark, Søltofts Plads 228A, Kgs., Lyngby 2800, Denmark

<sup>c</sup> Department of Physics, Chemistry, and Pharmacy, University of Southern Denmark, Campusvej 55, Odense M 5230, Denmark

<sup>d</sup> Aalborg Univ, Center Microbial Communities, Department of Chemistry and Bioscience, Fredrik Bajers Vej 7, H, 3-503, 9220 Aalborg, Denmark

## ARTICLE INFO

### Keywords:

Biofilm composition  
MABR  
Redox  
IFAS  
Elemental composition  
16s rRNA

## ABSTRACT

Membrane-Aerated Biofilm Reactors (MABRs) are becoming a popular process intensification alternative within wastewater treatment plants (WWTP). Indeed, the nitrogen removal capacity of aerobic/anoxic/anaerobic reactors can be substantially enhanced with reduced energy consumption and footprint requirements. However, little is known about how oxidation-reduction potential (ORP) may impact their overall process performance. This study aims to report some of these effects by showing the results of almost three years of monitoring of two hybrid MABRs (R1, R2) adjacent to an existing Biotenipho™ facility. In Period 1 (P1), R1 and R2 were fed with anaerobic mixed liquor from the selector for the biological phosphorus removal zone. In Period 2 (P2), external aeration was introduced to increase ORP values (R1, R2), and membranes were replaced (R1) or cleaned (R2). Results show an increase in nitrification rates: from 0.27 and 0.33 g N m<sup>-2</sup> d<sup>-1</sup> in R1/R2 during P1 to 1.0 and 0.80 g N m<sup>-2</sup> d<sup>-1</sup> in R1/R2 during P2. 16 s rRNA amplicon sequencing analysis revealed that the relative abundance of nitrifying organisms increased from 0.2 to 6.7 % in R1 and 0.8 to 5.3 % in R2 in P2 (in detriment of microbes with fermenting capabilities). Energy dispersive X-ray spectroscopy confirmed the presence of coating substances under the lowest ORP (P1), which could be pyrite and its precursors like mackinawite. Overall, it is hypothesized that low ORP conditions (P1) had a detrimental effect on nitrification performance, as it promoted the reduction of different iron and sulfur compounds, which in turn a) precipitate in the biofilm as FeS increasing mass transfer limitations and competing with biomass for space; b) re-oxidize increasing the internal oxygen demand; c) inhibit nitrifiers growth.

## 1. Introduction

Wastewater treatment plants are often required to increase their treatment capacity due to population growth, industrial contributions, or changes in legislation, among others. While infrastructure expansion might be necessary under specific circumstances, constructing new (typically concrete-made) bioreactors to increase capacity is generally avoided due to the high economic, social, and environmental costs of building additional reactor volume [83].

Membrane aerated biofilm reactors (MABRs), which rely on membranes capable of transferring oxygen across the membrane to support biofilm growth [7], can increase nitrogen removal in existing

bioreactors while significantly reducing energy consumption [61,8,81]. The use of MABR in combination with suspended growth (activated sludge) is usually referred to as a “hybrid MABR” technology [16]. In this type of system, heterotrophic organisms grow in the suspended fraction, using the nitrite (NO<sub>2</sub><sup>-</sup>) and nitrate (NO<sub>3</sub><sup>-</sup>) produced within the nitrifying biofilm, providing some advantages: nitrification resilience to increases in biological oxygen demand loadings [16,62] and the ability to perform simultaneous nitrification-denitrification in a single reactor without nitrate recirculation [6]. Moreover, biomass sloughing from the MABR biofilm into the suspended fraction has been shown to reduce the suspended growth solids retention time below minimum design values while maintaining full nitrification capabilities [30,12].

Because of the reduced substrate diffusivity to the biofilm compared

\* Corresponding author at: Vandcenter Syd A/S, Vandværksvej 7, Odense 5000, Denmark.

E-mail address: [neca@kt.dtu.dk](mailto:neca@kt.dtu.dk) (N. Uri-Carreño).

<https://doi.org/10.1016/j.cej.2022.138917>

Received 14 May 2022; Received in revised form 12 August 2022; Accepted 26 August 2022

Available online 5 September 2022

1385-8947/© 2022 The Author(s). Published by Elsevier B.V. This is an open access article under the CC BY license (<http://creativecommons.org/licenses/by/4.0/>).

Nomenclature			
A	Membrane surface area, m <sup>2</sup>	NO <sub>3</sub> <sup>-</sup>	Nitrate, g N/m <sup>-3</sup>
CA	Correspondance Analysis	NR	Nitrification rate, g N/m <sup>-2</sup> d <sup>-1</sup> or g O <sub>2</sub> m <sup>-3</sup> d <sup>-1</sup>
fCOD	Filtered Chemical Oxygen Demand, g COD m <sup>-3</sup>	O <sub>2,exh</sub>	Oxygen concentration in the exhaust gas after membranes, %
DPAO	Denitrifying Polyphosphate-Accumulating Organism	ORP <sub>inf/eff</sub>	Oxidation-Reduction Potential in the influent and effluent, mV
EA	External aeration, supplementary fine bubble aeration in the reactor, m <sup>3</sup> /h	OTR	Oxygen Transfer Rate, g O <sub>2</sub> m <sup>-2</sup> d <sup>-1</sup> or g O <sub>2</sub> m <sup>-3</sup> d <sup>-1</sup>
EBPR	Enhanced Biological Phosphorus Removal	OTU	Operational Taxonomic Unit
EDX	Energy dispersive X-ray spectroscopy	P1/P2/ P2a/P2b	Study periods 1, 2, 2a and 2b
Fe <sub>dis</sub>	Iron concentration g Fe m <sup>-3</sup>	PAO	Polyphosphate-Accumulating Organism
Fe <sup>2+</sup>	Ferrous ion	PCA	Principal Component Analysis
Fe <sup>3+</sup>	Ferric ion	PO <sub>4</sub> <sup>3-</sup>	Phosphate, g P/m <sup>-3</sup>
FeS	Iron sulfide	Q <sub>inf</sub>	Feed flow to the MABR reactor, m <sup>3</sup> /h
FeSO <sub>4</sub>	Ferric sulfate	R1/R2	MABR reactors 1 and 2
H <sub>2</sub> S/HS <sup>-</sup>	Sulfide	S <sub>0</sub> /SO <sub>x</sub>	Sulfur/sulfur oxides
HFO	Hydrous Ferric Oxides	SEM	Scanning Electron Microscope
ICP-OES	Inductively Coupled Plasma-Optical Emission Spectrometry	SO <sub>4</sub> <sup>2-</sup>	Sulfate concentration, g/m <sup>-3</sup>
IRB	Iron-reducing bacteria	SOB	Sulfur-oxidizing bacteria
K <sub>i</sub>	Inhibition constant, g S m <sup>-3</sup>	SRB	Sulfur-reducing bacteria
MABR	Membrane Aerated Biofilm Reactor	T	Temperature
NH <sub>x, inf/eff</sub>	Ammonia/um concentration in the influent/effluent g N/m <sup>-3</sup>	V <sub>loss</sub>	Volumetric air loss between inlet and outlet
NH <sub>x,i,inf</sub>	Ammonia/um load in the influent, g N/m <sup>-2</sup> d <sup>-1</sup>	VSS	Volatile suspended solids
NO <sub>2</sub> <sup>-</sup>	Nitrite, g N/m <sup>-3</sup>	Xo <sub>2,in/out</sub>	Mol fraction of oxygen in atmospheric air and the MABR exhaust
		ρ <sub>o2</sub>	Oxygen density under normal conditions, kg/m <sup>-3</sup>

to a suspended growth system, integrated fixed-film activated sludge systems, such as hybrid MABRs, should ideally be located in a bioreactor where the ammonia/ammonium (NH<sub>x</sub>) concentrations are high [20]. Moreover, the soluble chemical oxygen demand (COD) loading should be low enough so that faster-growing heterotrophic organisms do not outcompete nitrifiers in the biofilm [29].

Besides NH<sub>x</sub> and COD concentrations, another critical aspect to consider is the oxidation–reduction potential (ORP) in the given reactor since oxygen in counter-diffusional biofilms, diffuses from the biofilm base and oxygen gradients play an important role in nitrogen removal [16,2,47]. Previous studies have focused on the feasibility of hybrid MABRs in anoxic zones and showed it provides significant benefits [77,25,6]. However, the current layout of some treatment facilities lacks strictly anoxic zones -e.g., phase-isolation oxidation ditches-based processes (BioDenitro™) or configurations based on sequencing batch reactors. In this case, anaerobic zones for enhanced biological phosphorus removal (EBPR) might seem like a logical alternative to anoxic zones to place MABRs, because of the high NH<sub>x</sub> and low oxygen concentrations in these reactors. To the best of our knowledge, there is currently no information regarding the implications of choosing an anaerobic zone for a hybrid MABR application and how anaerobic conditions, low ORP, might impact the nitrogen removal performance in such a hybrid MABR.

In a previous study by [81], ORP was identified as strongly correlated to nitrification rates. The lower the ORP, the lower the nitrification rates. In this study, we monitored two pilot-scale hybrid MABRs fed with mixed liquor from an anaerobic zone from an existing EBPR bioreactor (mixture of return activated sludge and primary effluent), and we analyzed the impact of different ORP conditions on the overall process performance. The reactors were operated for approximately-three years in total. The study time was divided into two periods (P1 and P2), which corresponded with the addition of external aeration (EA) in the form of fine bubble aeration. The latter allowed to increase ORP levels by injecting oxygen within the bulk. The biofilm's elemental and microbial composition was analyzed from samples taken before and after introducing EA 1) using a scanning electron microscopy coupled with energy dispersive X-ray spectroscopy (SEM-EDX), 2) inductively coupled

plasma-optical emission spectrometry (ICP-OES), and 3) 16 s rRNA amplicon sequencing. Results from this study indicate that very low ORP levels in combination with the presence of Fe and S compounds should be considered when designing hybrid MABR applications to avoid the potentially detrimental consequences for nitrification performance observed in this study.

## 2. Methods

### 2.1. Mabrs setup

The Ejby Mølle Water and Resource Recovery Facility in Odense, Denmark, has a 410,000 population equivalents treatment capacity. The main liquid treatment train is comprised of grit removal and screening (6 mm), chemically enhanced primary treatment with the addition of polymers and ferric sulfate (FeSO<sub>4</sub>), and Bio-Denipho™ nutrient removal with phased-isolated oxidation ditches, including anaerobic zones for EBPR and tertiary treatment with sand filters. Further details on the plant have been reported by [81] and a more detailed flowchart than that in Fig. 1 can be found in Fig S1.

The MABR tanks consisted of two sidestream circular reactors of 23 m<sup>3</sup> (R1) and 18 m<sup>3</sup> (R2) each, adjacent to the EBPR bioreactor facility's anaerobic zone (Fig. 1). Two full-scale hollow-fiber MABR units with a total volume of 11.3 m<sup>3</sup> and 4.5 m<sup>3</sup> and a total membrane surface area of 1920 m<sup>2</sup> and 1450 m<sup>2</sup> were installed inside Reactor 1 (R1) and 2 (R2) in 2018. The reactors were set up as continuously stirred-tank reactors fed with mixed liquor from the full-scale anaerobic zones (i.e., primary effluent mixed with return activated sludge). The feed was pumped from the anaerobic zone and introduced to the tanks near the bottom using a distribution grid. The effluent was located at the top of the tanks.

Low-pressure air was supplied to the MABR units for intramembrane oxygen supply. Additional air was supplied for biofilm scouring, a process carried out differently in R1 and R2 according to the manufacturer's instructions. Process and scouring airflows to the MABR were adjusted manually. Pressure before and after the units was measured using a pressure transmitter connected to the supervisory control and data

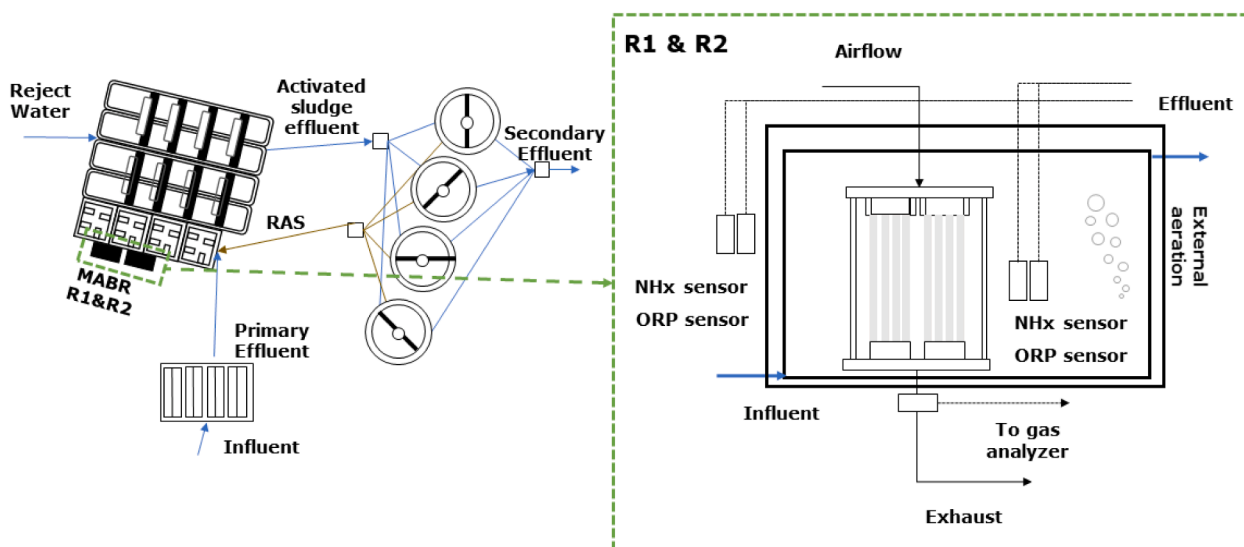


**Fig. 1.** LEFT: Simplified flow diagram of Ejby Mølle WRRF: influent/raw wastewater, primary settlers, input to EBPR anaerobic section, input to MABR1 (R1) and MABR (R2), reject water stream, oxidation ditch, secondary settlers, treated effluent, return activated sludge stream (RAS). RIGHT: Schematic of MABR R1 and R2 showing: membranes, influent, effluent,  $\text{NH}_x$  and ORP sensor locations, airflow inlet and exhaust and external aeration.

acquisition system. Airflow before the MABR was measured using an analog rotameter; therefore, the process airflow values were recorded manually. Different probes were used to continuously monitor the liquid phase in the influent and the MABR reactor.  $\text{NH}_x$  concentrations and temperature (T) were measured using an AmmoLyt® plus device, and ORP was measured using a SensoLyt® ORP probe, both from Xylem Inc. A sample from the exhaust gas after the MABR unit was taken semi-continuously to a gas-monitoring GASloq 1200 from ABB Group A/S. The system contained a gas analyzer Uras 26 Easyline and was designed to operate as a multi-scan and measuring point analysis system with

oxygen ( $\text{O}_{2,\text{exh}}$ ) measurement. A general schematic applicable to both R1 and R2 can be found in Fig. 1 (right).

## 2.2. Operational periods

The two MABR reactors were operated for approximately three years (June 2018–March 2021). Fig. 2 shows the different periods of operation during the study: P1 (508 days), before the introduction of EA in the reactors (in pink); P2, after the EA came into operation (in yellow/green). In Reactor 1 (R1), the original membranes were replaced by new

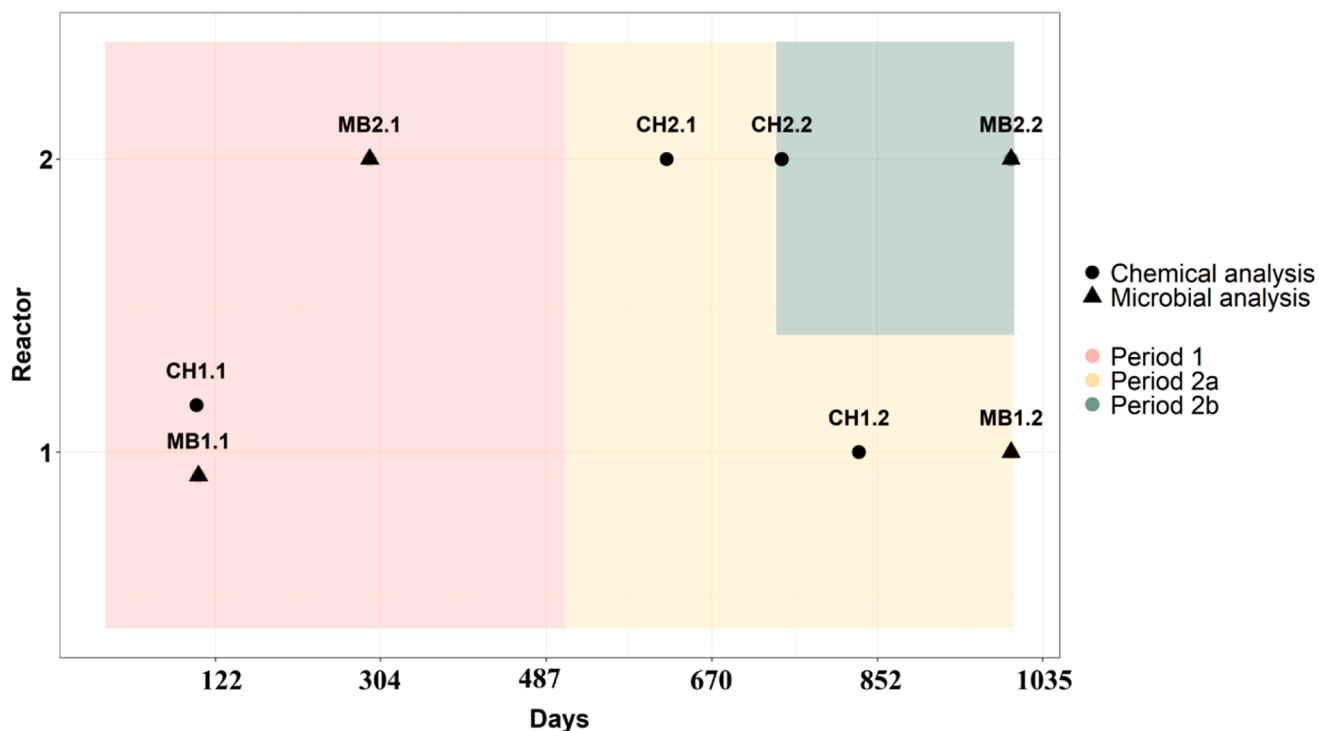


**Fig. 2.** A chronological display of study periods and collection of samples for chemical and microbial analysis. Circles and triangles correspond to the acquisition of samples for chemical and microbial analysis, respectively, while colors indicate periods P1 (pink), P2 and 2a (yellow), and P2b (green). Reactor number in the y axis. (For interpretation of the references to color in this figure legend, the reader is referred to the web version of this article.)

ones at the beginning of P2. In Reactor 2 (R2), P2 is further divided into P2a (254 days) and P2b (242 days), which indicates a chemical cleaning of the membranes and the introduction of an improved mixing system (green) respectively. More details can be found in Table S4.

The EA was provided with fine bubble diffusers on one side of the tank in P2 to increase the redox conditions inside the reactors. The EA was operated intermittently and controlled using two strategies: time-based control during the first three months and an ORP-based feedback control during the study's remainder. The ORP-based feedback control also included managing the feed flow to the tank: decreasing the flow when the ORP reached a pre-defined low setpoint. More details on operation during the different periods can be found in Table 2. Spot measurements were carried out to ensure EA oxygen supply was insufficient to provide significant dissolved oxygen levels in the reactors. Moreover, batch tests without using EA were performed periodically to ensure NR with and without EA were not significantly different [81].

### 2.3. Analytical methods

Time-proportional composite samples (24 h) and grab samples from both the feed and the pilot reactor's interior were collected regularly and analyzed throughout the study. The concentrations of  $\text{NH}_x$ ,  $\text{NO}_2^-$ ,  $\text{NO}_3^-$ , phosphate ( $\text{PO}_4^{3-}$ ), dissolved iron ( $\text{Fe}_{\text{dis}}$ ), sulfate ( $\text{SO}_4^{2-}$ ), and filtered chemical oxygen demand (fCOD) were measured using NANO-COLOR standard tests and a spectrophotometer NANOCOLOR UV/VIS II (Macherey – Nagel Inc.).

### 2.4. Performance indicators

The oxygen transfer rate (OTR) measures the flux of oxygen gas that diffuses from the lumen's interior into the biofilm over time. The calculation of OTR ( $\text{g O}_2 \text{ m}^{-2} \text{ d}^{-1}$ ) was based on the exhaust oxygen model reported in [29] (Eqs. (1a), (1b), (2)):

$$\text{OTR} = \frac{Q_{\text{air},\text{in}} (x_{\text{O}_2,\text{in}} - V_{\text{loss}} x_{\text{O}_2,\text{out}}) \rho_{\text{O}_2}}{A} \quad (1a)$$

$$\text{OTR} = \frac{Q_{\text{air},\text{in}} (x_{\text{O}_2,\text{in}} - V_{\text{loss}} x_{\text{O}_2,\text{out}}) \rho_{\text{O}_2}}{V} \quad (1b)$$

$$V_{\text{loss}} = \frac{1 - x_{\text{O}_2,\text{in}}}{1 - x_{\text{O}_2,\text{out}}} \quad (2)$$

Where  $Q_{\text{air},\text{in}}$  is airflow ( $\text{N m}^3 \text{ d}^{-1}$ ),  $x_{\text{O}_2,\text{in}}$  is the mole fraction of oxygen in atmospheric air,  $V_{\text{loss}}$  is the volumetric air loss between inlet and outlet,  $x_{\text{O}_2,\text{out}}$  is the mole fraction of oxygen in the exhaust.  $\rho_{\text{O}_2}$  is the oxygen density under normal conditions ( $\text{kg m}^{-3}$ ),  $A$  is the membrane surface area ( $\text{m}^2$ ), and  $V$  is the MABR unit volume (total volume occupied by the frame of the MABR unit) in  $\text{m}^3$ .

Nitrification rates (NR) represent the quantity of  $\text{NH}_x$  oxidized to  $\text{NO}_x$ . It was calculated using  $\text{NH}_x$  concentrations from the  $\text{NH}_x$  sensor (NR) as in Eqs. (3a), (3b) where  $\text{NH}_{x,\text{inf}}$  and  $\text{NH}_{x,\text{eff}}$  ( $\text{g m}^{-3}$ ), respectively, represented the concentration of  $\text{NH}_x$  in influent and effluent obtained from online signals and  $Q_{\text{inf}}$  was the influent flow rate ( $\text{m}^3 \text{ d}^{-1}$ ). More information about process indicators calculation methods can be found in [81].

$$\text{NR} = \frac{(\text{NH}_{x,\text{inf}} - \text{NH}_{x,\text{eff}}) Q_{\text{inf}}}{A} \quad (3a)$$

$$\text{NR} = \frac{(\text{NH}_{x,\text{inf}} - \text{NH}_{x,\text{eff}}) Q_{\text{inf}}}{V} \quad (3b)$$

### 2.5. Biofilm sampling

Biofilm samples were collected throughout the study period, according to Fig. 2. Sample collection from the full-scale MABR units

required lifting the units using a crane brought on-site specifically for this purpose. Membrane samples were collected by cutting membranes and “knotting” the open ends. Subsequent studies should ensure samples are collected in different locations throughout the MABR units to enhance the samples' representability, although this might not always be feasible in full-scale installations. Two samples from the suspended growth fraction in R1 and R2 (MB0) were taken simultaneously to MB1.2, and MB2.2 (Fig. 2). Samples were labeled and kept at  $-5^\circ\text{C}$  for chemical analysis and  $-80^\circ\text{C}$  for microbial analysis.

### 2.6. Elemental analysis of the biofilms

The morphological and elemental properties of the biofilm were investigated using a SEM (FEI Quanta 200, Netherlands) equipped with an Energy Dispersive Spectrometer (EDAX, Ametek, USA). The biofilm sample was dispersed in MilliQ water, dropped on a small piece of silicon wafer, and dried on a hot plate at  $50^\circ\text{C}$  prior to SEM-EDX analysis at low vacuum. Elemental mapping was collected to examine the presence of mineral particles in the sample. The elemental composition of these particles was further analyzed by EDX. To determine the absolute concentrations of elements relevant to inorganic precipitates in the biofilm, 0.02 g of CH1.2 (see Fig. 2) was mixed with 10 ml of 65 % nitric acid ( $\text{HNO}_3$ , Emsure-Merck KGaA) for microwave-assisted acid digestion ( $200^\circ\text{C}$  for 15 min). For samples CH1.1, CH2.1, and CH2.2, the precipitates were digested together with the membrane. After digestion and cooling, the supernatant of the digestate was diluted 10–100 fold for elemental analysis of P, Fe, Ca, Mg, and Al using an ICP-OES (Optima 2100 DV, PerkinElmer, USA).

### 2.7. Microbial analysis of the biofilms

DNA extraction, sample preparation, including amplification of V1-3 region of 16S rRNA gene using the 27F (AGAGTTTGATCCTGGCTCAG) [40] and 534R (ATTACCGGGCTGCTGG) [53] primers, and amplicon libraries were conducted as described by Stokholm-Bjerregaard et al., [72]. The V1-3 region was chosen for activated sludge community analysis, based on the studies by Albertsen et al., 2016 and [18], showing this primer to give the most representative community structure and the highest taxonomic resolution. Sequencing libraries were prepared by subsequent barcoding the V1-3 amplicon libraries with Nanopore-compatible custom adapters using 12.5  $\mu\text{L}$  PCR BIO 2X Ultra Mix, 1  $\mu\text{L}$  unique dual (UD) index adapter at ten  $\mu\text{M}$  (for a final adapter concentration of 400  $\mu\text{M}$ ), 2  $\mu\text{L}$  purified amplicon (at  $\sim 5 \text{ ng}/\mu\text{L}$ ) and 9.5  $\mu\text{L}$  nuclease-free water. The PCR program for the library PCR was  $95^\circ\text{C}$  for 2 min, eight cycles of  $95^\circ\text{C}$  for 20 s,  $55^\circ\text{C}$  for 30 s,  $72^\circ\text{C}$  for 60 s and a final elongation at  $72^\circ\text{C}$  for 5 min. The sequencing libraries were purified using CleanNGS beads (CleanNA, Netherlands) in a sample/bead ratio of 5/4. The sequencing libraries were multiplexed and adapted for Nanopore sequencing based on a custom ligation protocol based on the Sequencing Kit (SQK-LSK109); end-prep was performed by adding 3.5  $\mu\text{L}$  Ultra II End-prep reaction buffer and 1.5  $\mu\text{L}$  Ultra II End-prep enzyme mix (New England Biolabs, USA) to 25  $\mu\text{L}$  sequencing library. The end-prep reaction was incubated at  $20^\circ\text{C}$  for 5 min,  $65^\circ\text{C}$  for 5 min and then placed on ice for 30 s. Nanopore adapters were ligated on by adding 5  $\mu\text{L}$  Adapter Mix (AMX from the SQK-LSK109 kit, Oxford Nanopore Technologies, UK), 40  $\mu\text{L}$  Ultra II Ligation master mix and 1  $\mu\text{L}$  Ultra II Ligation enhancer (New England Biolabs, USA) and incubating at room temperature for 10 min. The Nanopore sequencing libraries were purified using CleanNGS beads (CleanNA, Netherlands) in a sample/bead ratio of 2/1. The libraries were loaded onto a MinION 106 v.9.4.1 flowcell in a MinION Mk1C sequencer (Oxford Nanopore Technologies, UK) according to the manufacturer's protocol. Live base-calling was enabled using Guppy 3.6.0 (Oxford Nanopore Technologies, UK) with the fast model. The base-called fastq files were processed using a custom shell script available at <https://github.com/martinhjorth/onlineDNA-workflow>. The fastq files were trimmed and demultiplexed



**Table 1**

Average values and standard deviation for influent and effluent characteristics at the different study periods for R1 and R2 combined.

		$\text{SO}_4^{2-}$ $\text{g/m}^{-3}$	$\text{Fe}_{\text{dis}}$ $\text{g/m}^{-3}$	$\text{NH}_x$ $\text{g N/m}^{-3}$	fCOD $\text{g COD m}^{-3}$	$\text{PO}_4^{3-}$ $\text{g P/m}^{-3}$	$\text{NO}_2^-$ $\text{g N/m}^{-3}$	$\text{NO}_3^-$ $\text{g N/m}^{-3}$	COD/N
P1	Influent	85 ± 5	4.9	19.5 ± 8.7	69 ± 25	16.3 ± 8.7	–	–	3.5
	Effluent	74 ± 4	0.1	15.5 ± 8.2	56 ± 21	8.8 ± 8.0	0.0 ± 0.1	0.4 ± 0.4	
	% Reduction	12 ± 7 %	98 %	21 ± 30 %	17 ± 29 %	50 ± 38 %	–	–	
P2	Influent	95 ± 13	2.2 ± 1.5	15.5 ± 6.5	53 ± 18	19.1 ± 11.5	–	–	3.4
	Effluent	94 ± 21	0.4 ± 0.4	11.4 ± 6.3	47 ± 13	8.3 ± 7.3	0.0 ± 0.1	0.6 ± 1.3	
	% Reduction	2 ± 15 %	66 ± 33 %	35 ± 18 %	18 ± 11 %	57 ± 23 %	–	–	

using cutadapt v. 2.8 [49]; first, to find the outer custom adapters used (CAGAAGACGGCATACGAGAT...GTGTAGATCTCGGTGGTCGC), retaining only amplicons between 275 and 450 bp, accepting a 20 % error rate and a minimum overlap of 10 bp. Barcodes (inner custom adapters) were subsequently trimmed off using the same settings, and demultiplexed fastq files were output. The demultiplexed reads were mapped to MiDAS 3.7 [57] using minimap2 v. 2.17 [42], and the mappings were filtered based on SAM flags using SAMtools v. 1.10 [43], removing flags 4 (unmapped), 256 (non-primary) and 2048 (supplementary). The mappings were loaded into the R environment v. 3.5.0 [64] and processed using the data.table, dplyr [89] and tidyr packages [88]. The mappings were filtered to retain alignments covering >85 % of the references and output as a 'txt' file containing the alignments. Operational and sequencing data were analysed and visualized in the R environment (v. 4.1.0) [64] using RStudio [65] with the ampvis2 package (v. 2.7.5 [4] <https://paperpile.com/c/apGkha/i1ao>) and the tidyverse (v. 1.3.1 [88]). Sequencing data and R scripts are available on request.

### 3. Results

#### 3.1. Chemical analysis of influent and effluent

Results from influent and effluent characteristics obtained from off-line laboratory samples can be seen in Table 1. Influent was taken from an EBPR zone containing a mixture of return activated sludge and primary settling effluent, and therefore after the addition of  $\text{FeSO}_4$ . The mixed liquor concentration was, on average, 5000 mg/L. This influent sample was assumed to represent both R1 and R2 since feed to both reactors is pumped from the same EBPR zone. Effluent results are a combination of samples taken from both R1 and R2. In general, high variability in the results can be observed, and only few samples from P1 could be analyzed for  $\text{SO}_4^{2-}$  and  $\text{Fe}_{\text{dis}}$ .  $\text{Fe}_{\text{dis}}$  and  $\text{SO}_4^{2-}$  conversion rates decreased (from 98 % to 66 ± 33 % and from 12 ± 7 % to 2 ± 15 %) from P1 to P2. The  $\text{NH}_x$  removal rate increased from 21 ± 30 % to 35 ±

18 %, and the removal of  $\text{PO}_4^{3-}$  increased from 50 ± 38 % to 57 ± 23 %. Removal of fCOD was 17 ± 29 % and 18 ± 11 %. The concentrations of  $\text{NO}_2^-$  and  $\text{NO}_3^-$  remained very low during the whole study period, 0.1 ± 0.1 and 0.4 ± 0.4 g N m<sup>-3</sup> in P1 and 0.0 ± 0.1 and 0.6 ± 1.3 g N m<sup>-3</sup> in P2, respectively.

#### 3.2. Online sensors based performance

Results in this section are expressed per unit of membrane area (Eq 2a,3a), but results expressed per volume unit of the MABR (Eq 2b, 3b) can also be seen in Table 2. During P1 (first 508 days), the low ORP conditions of the feed resulted in low ORP conditions inside the MABR reactors (see Fig. 3). As shown in Table 2, the  $\text{ORP}_{\text{eff}}$  was on average  $-264 \pm 152$  and  $-269 \pm 126$  mV inside R1 and R2, respectively. During this period, NR in the reactors was very low, with average values of  $0.27 \pm 0.52$  and  $0.33 \pm 0.49$  g N m<sup>-2</sup> d<sup>-1</sup>; while OTR averaged  $7.52 \pm 2.41$  and  $8.60 \pm 2.68$  g O<sub>2</sub> m<sup>-2</sup> d<sup>-1</sup>. The ratio between OTR and NR was 18 ± 14 and 21 ± 15 g O<sub>2</sub> g N<sup>-1</sup>, respectively. Based on stoichiometry, the expected ratio would be 4.57 if all O<sub>2</sub> was used to convert  $\text{NH}_x$  to  $\text{NO}_3^-$ .

P2 was characterized by the introduction of EA in the reactors (fine bubble diffusers), first controlled using an open-loop controller (timer) and afterward using a feedback on/off controller based on the ORP signal in the tanks. The  $\text{ORP}_{\text{eff}}$  increased to  $-171 \pm 87$  in R1 and to  $-136 \pm 65$  and  $-210 \pm 101$  in R2 (see Table 2). The ORP in the feed ( $\text{ORP}_{\text{inf}}$ ) was, on average  $-373 \pm 30$  and  $-404 \pm 72$  mV during P1 and P2, respectively (see Table 2). The  $\text{NH}_x$  load in P2 was increased from  $1.49 \pm 1.06$  and  $1.65 \pm 1.26$  to  $2.98 \pm 1.44$  and  $2.63 \pm 1.45$  g N m<sup>-2</sup> d<sup>-1</sup> in R1 and R2, respectively.

The nitrification performance in R1 significantly increased during P2 (p-value < 0.01), achieving an average NR of  $1.01 \pm 0.57$  g N m<sup>-2</sup> d<sup>-1</sup> and average OTR of  $9.20 \pm 2.27$  g O<sub>2</sub> m<sup>-2</sup> d<sup>-1</sup> (see Table 2). The OTR/NR ratio was reduced to  $11.22 \pm 8.78$  g O<sub>2</sub> g N<sup>-1</sup>.

For R2, the introduction of EA (P2a) increased NR from  $0.33 \pm 0.49$  to  $0.59 \pm 0.42$  g N m<sup>-2</sup> d<sup>-1</sup> while OTR decreased from  $8.60 \pm 2.68$  to  $3.68 \pm 2.19$  g O<sub>2</sub> m<sup>-2</sup> d<sup>-1</sup>. A change in operation can explain this

**Table 2**Summary of performance data grouped by reactor and period. Statistical significance of the distributions per period compared to the overall distribution for each reactor using a *t*-student test are indicated in bold (p-value < 0.001) and italics (p-value < 0.05).

			Duration	T	$\text{NH}_{x,\text{inf}}$	$\text{NH}_{x,\text{eff}}$	$\text{ORP}_{\text{inf}}$	$\text{ORP}_{\text{eff}}$	EA	OTR		NR		OTR/NR
			days	°C	$\text{g N m}^{-2} \text{d}^{-1}$	$\text{g N m}^{-3}$	mV	mV	$\text{m}^3 \text{h}^{-1}$	$\text{g O}_2 \text{m}^{-2} \text{d}^{-1}$	$\text{g O}_2 \text{m}^{-3} \text{d}^{-1}$	$\text{g N m}^{-2} \text{d}^{-1}$	$\text{g N m}^{-3} \text{d}^{-1}$	$\text{g O}_2 \text{g N}^{-1}$
R1	P1	508	16	16	1.49 ±	16.45 ±	−373 ±	−264 ±	0	7.52 ±	1277.59 ±	0.27 ±	45.87 ±	18.14 ±
					± 3	<b>1.06</b>	<b>8.63</b>	<b>30</b>		<b>2.41</b>	<b>326.23</b>	<b>0.52</b>	<b>88.35</b>	<b>14.40</b>
R1	P2	491	14	± 3	2.98 ±	10.12 ±	−404 ±	−171 ±	5 ± 5	9.20 ±	1563.76 ±	1.01 ±	171.61 ±	11.22 ±
					1.44	5.79	72	87		2.27	385.70	0.57	<b>96.85</b>	8.78
R2	P1	506	16	± 3	1.65 ±	16.75 ±	−373 ±	−269 ±	0	8.60 ±	2771.64 ±	0.33 ±	104.02 ±	20.65 ±
					1.26	12.91	30	126		2.68	845.37	0.49	154.46	15.36
R2	P2a	233	13	± 2	2.63 ±	9.05 ±	−374 ±	−136 ±	14 ±	3.68 ±	1186.32 ±	0.59 ±	154.46 ±	8.15 ±
					1.45	<b>4.35</b>	<b>30</b>	<b>65</b>		<b>2.19</b>	691.55	0.42	132.39	<b>9.57</b>
R2	P2b	224	16	± 3	2.55 ±	12.17 ±	−464 ±	−210 ±	4 ± 4	10.52 ±	3389.36 ±	0.80 ±	283.70 ±	14.11 ±
					<b>1.18</b>	5.71	<b>35</b>	<b>101</b>		<b>4.86</b>	<b>1531.71</b>	<b>0.52</b>	163.91	10.85

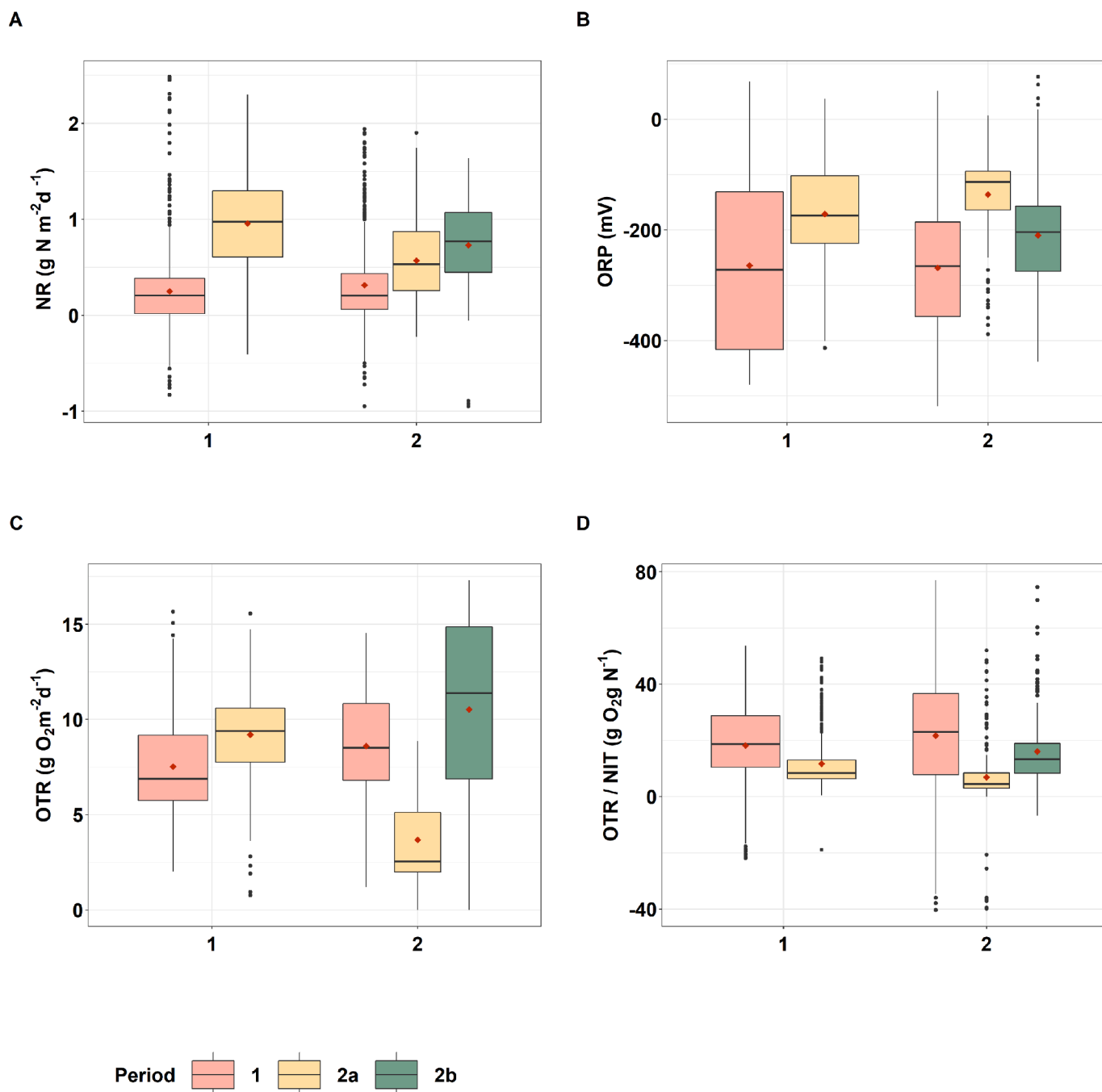


Fig. 3. Boxplots containing results for NR (A),  $\text{ORP}_{\text{eff}}$  (B), OTR (C), and OTR/NR ratio (D), for Reactor 1 and 2 (X-axis), grouped by period: P1, P2a, and P2b.

decrease in OTR: During this period, the intramembrane process airflow was reduced to increase the difference between inlet and outlet  $\text{O}_2$  concentrations and increase the accuracy of OTR estimations. Moreover, the use of EA in this period was high ( $14 \text{ m}^3/\text{h}$  compared to  $4 \text{ m}^3/\text{h}$  in P2b and  $5 \text{ m}^3/\text{h}$  in R1). In this period, the OTR/NR ratio was further reduced to  $8 \pm 10 \text{ g O}_2 \text{g N}^{-1}$  (see Fig. 3). However, it was after the chemical cleaning of the biofilm and the introduction of an improved mixing strategy (P2b) that the NR and OTR significantly improved, to average values of  $0.80 \pm 0.52 \text{ g N m}^{-2} \text{d}^{-1}$  and  $10.52 \pm 4.86 \text{ g O}_2 \text{m}^{-2} \text{d}^{-1}$ . The reader must be aware that only  $\text{NH}_x$  concentrations were used in the calculations, and neither ammonification (mineralization of soluble organic nitrogen) nor biomass assimilation were included in the calculations. Mass balances based on total nitrogen were not possible to

carry out due to the high MLSS concentrations.

Fig. 4 shows the resulting biplots from multivariate analysis using PCA for both R1 (left) and R2 (right), while a summary of results can be seen in Table S3a,b,c and d (supplemental information). The two PCs (1 and 3) explain 55.7 % and 46.1 % of the variability in the data. The loadings of  $\text{ORP}_{\text{eff}}$  and NR are highlighted in blue, while points are colored according to P1 (pink) and P2 (yellow). Both biplots show  $\text{ORP}_{\text{eff}}$  and NR are positively correlated, and there was a transition from P1 to P2 from lower to higher  $\text{ORP}_{\text{eff}}$  and NR. Moreover, a correlation plot with Pearson's correlation values can be seen in Fig. S9 (supplemental information), showing NR was strongly and significantly correlated to  $\text{ORP}_{\text{eff}}$  values.



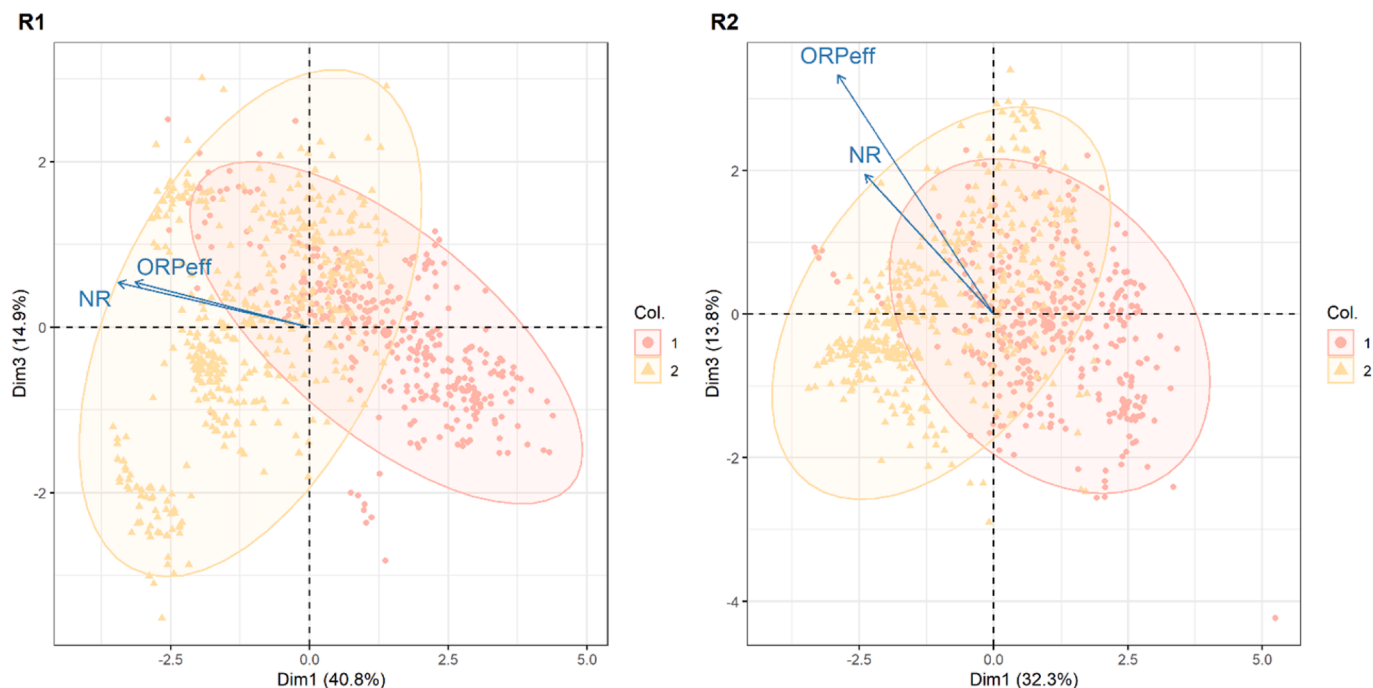


**Fig. 4.** Principal Components Analysis (PCA) of daily data from reactors 1 (left) and 2 (right). Points colored in pink correspond to period 1 and yellow to period 2. The selected variables  $ORP_{eff}$  and NR are shown in blue. (For interpretation of the references to color in this figure legend, the reader is referred to the web version of this article.)

### 3.3. Elemental composition of the biofilms

Results from the EDX analysis from R1 and R2 can be seen in Fig. 5. Results from ICP-OES analysis and molar ratios can be seen in Table S1 and S2. SEM images and EDX spectra can be seen in Figs. S2, S3, S4, and S5. The samples were a mixture of organic matter (e.g., microbes and extra polymeric substances as the backbone of biofilm) and inorganic precipitates: Fe, P, and Ca as the main constituents, e.g., Fe phosphate, Fe hydroxides (HFO) with  $PO_4^{3-}$  adsorbed, and Ca phosphate, to different extents.

Graph A in Fig. 5 shows the difference in the elemental composition of two membrane samples from R1, before (CH1.1) and after (CH1.2) the

introduction of EA and replacement of membranes. The P, Fe, Ca, and S content were 2, 37, 2, and 18 % in sample CH1.1, while in sample CH1.2, they were 11, 24, 10, and 0.1. For sample CH1.1, the contents of Fe (37 %) and S (18 %) were relatively high. This is supported by the mapping of C, Fe, and S signals over the sample particles (Fig. S2). Two areas with significant S signals were further analyzed, and the EDX results indicated high concentrations of Fe and S, with Fe:S ratios of 0.56 and 0.64. This suggests the possible presence of pyrite ( $FeS_2$ , Fe:S = 0.5) and/or its precursor mackinawite ( $FeS$ , Fe:S = 1) [46]. Images from membrane samples taken in P1 show indications of black coating (Fig. 6), strongly indicating the presence of an iron sulfide ( $FeS$ ) compound.

Graph B in Fig. 5 shows the difference in the chemical composition

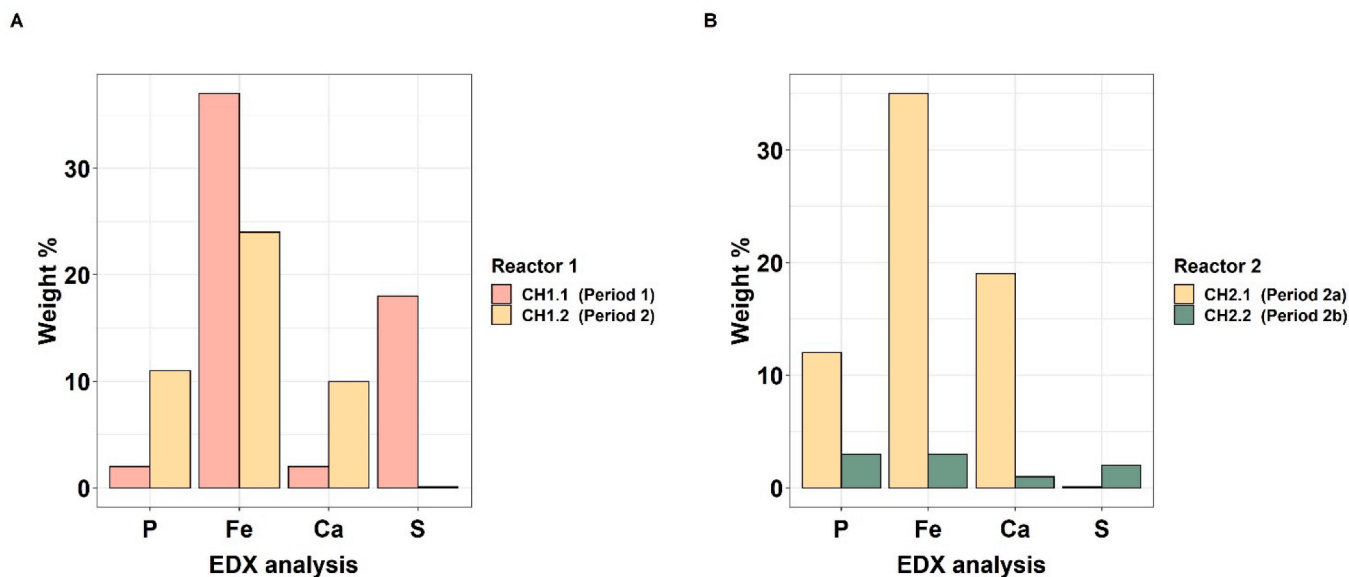


**Fig. 5.** Results from EDX analysis for R1 (A) and R2 (B). Chemical elements on the x-axis and percentage of weight in the sample on the y-axis.



Fig. 6. Membrane samples with a seemingly black coating from R1 and R2 sampled during P1.

between a sample taken before (CH2.1) and after (CH2.2) the chemical cleaning of R2. Hence, the percentage of P, Fe, and Ca dropped from 12, 35, and 19 to 3, 3, and 1, respectively. This is a clear indication that introducing the MABR membranes in an acidic environment successfully removed the inorganic precipitates present: Ca, Fe and P, leaving behind a biofilm composed primarily of organic matter. Sulfur mainly remained unchanged (0.1–2 wt%).

The elemental concentrations of P, Fe, Ca, Al, and Mg by ICP-OES analysis are summarized in Table S1. Overall, P, Fe, and Ca showed relatively high contents, while an insignificant amount of Al and Mg was observed. Fe showed a much higher range than the other four elements, consistent with the EDX analysis (Fig. 5).

The molar ratios of Fe:P, Ca:P, and Fe:Ca were calculated based on both EDX and ICP-OES results (Table S2). This can provide an insight into the elemental composition, especially for CH1.2, CH2.1, and CH2.2, in which only relative concentrations of P, Fe, and Ca were obtained. Some differences were observed between the values from EDX and ICP-OES, but a similar trend in the data was obtained. The differences should

be attributed to that EDX collects the elemental signals from the sample's surface, whereas ICP-OES measures the element's absolute (bulk) concentration in the whole sample. Here the discussion is based on the ICP-OES analysis. The Fe:Ca ratios of the samples were between 1.2 and 9.6, indicating a higher content of Fe than Ca in all precipitate samples. The highest molar ratios of Fe:P (12.7) and Fe:Ca (9.6) were found in CH1.1, which is consistent with its high content of Fe (Fig. 5 and Fig. S2). For the other three samples, comparable ratios of Fe:P (0.7–0.9), Ca:P (0.4–0.6), and Fe:Ca (1.2–1.8) were obtained. CH2.2 showed the lowest ratios of Fe:P (0.7) and Ca:P (0.4), and this is consistent with its low concentrations of Fe and Ca observed by EDX (Fig. 5).

### 3.4. MICROBIAL COMPOSITION OF THE BIOFILMS

Figs. 7 and 8 contain information about the 16 s rRNA analysis of samples taken from the MABR biofilm and the mixed liquor in the reactors. Samples from the biofilm in R1 were called MB1.1 (before EA)

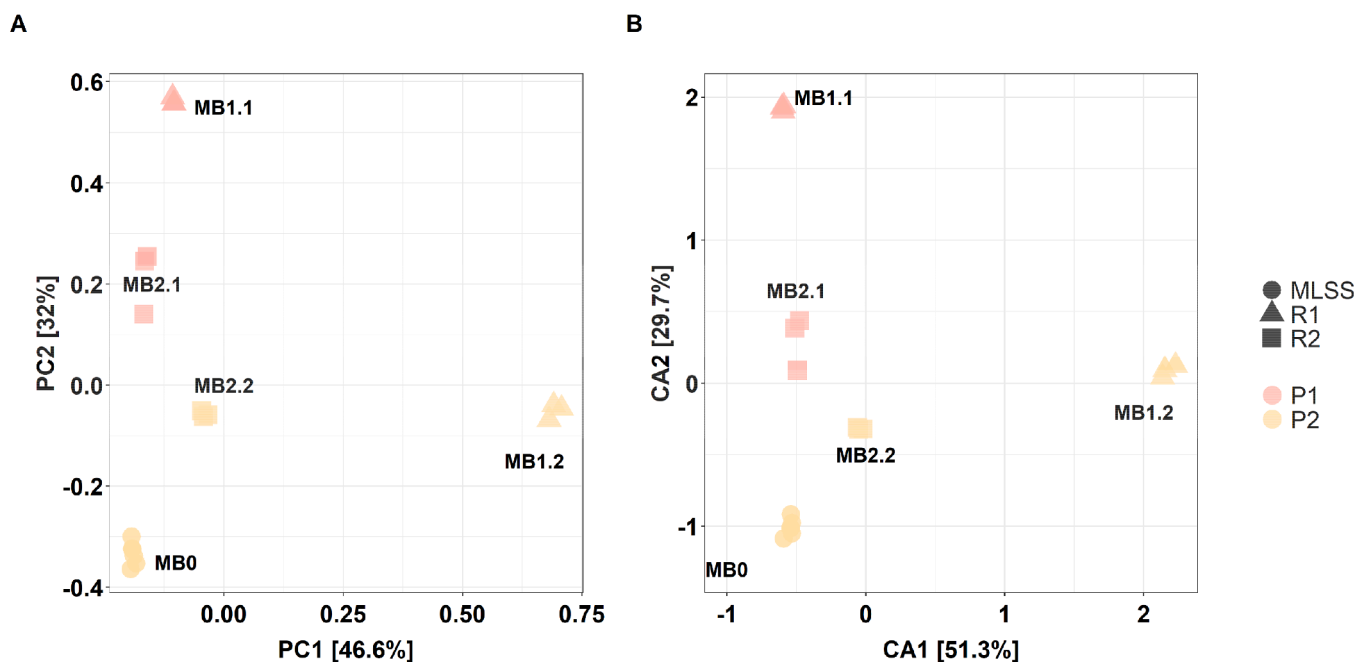
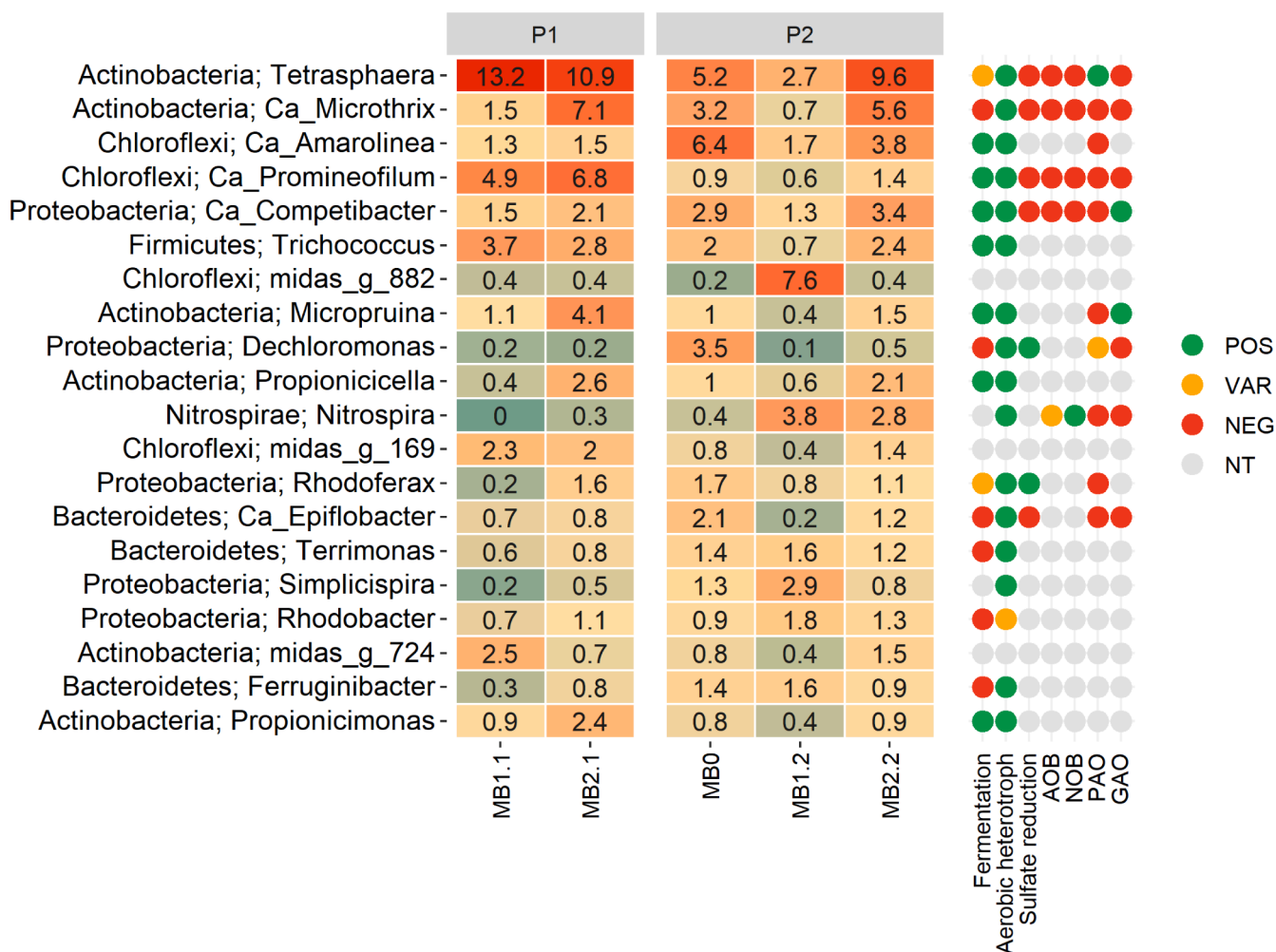


Fig. 7. Principal Components Analysis (PCA) (A) and Correspondence Analysis (CA) (B) of 18 samples and 485 OTUs. Before the analysis, OTUs present in <0.1% relative abundance in any sample have been removed. The data has been transformed initially by applying the Hellinger transformation (Legendre & Gallagher, 2001). Each axis's relative contribution (eigenvalue) to the total inertia in the data is indicated in percent at the axis titles.



**Fig. 8.** Heatmap of 20 most abundant Genera (by mean) grouped by period and by whether it corresponds to a mixed liquor sample (MB0) or a biofilm sample from Reactor 1(MB1.1 and MB1.2) and 2 (MB2.1 and MB2.2). Color guide on the right indicates whether the organism has a known function (POS as positive, NEG as negative, VAR as variable and NT as not assessed). This information was retrieved from [midasfieldguide.org](https://midasfieldguide.org).

and MB1.2 (after EA and new membranes) and in Reactor 2 MB2.1 (before EA) and MB2.2 (after EA and chemical cleaning). Sample MB0 (mixed liquor) corresponds to the average of two samples taken from the mixed liquor in R1 and R2, at the same time as MB1.2 and MB2.2 were taken from the respective biofilms. [Fig. 5](#), [Fig. S6](#), and [Fig. S7](#) show average values from the analysis of triplicate samples.

Results from both PCA and CA revealed two important messages: First, samples taken from R1 in the two different study periods (MB1.1 and MB1.2) present larger differences in microbial composition than R2. Secondly, samples taken in R2 were closer to each other (MB2.1 and MB2.2) and the mixed liquor samples (MB0). This can be seen in [Fig. 7](#), where points located close to each other represent similar microbial communities. In contrast, microbial communities are different when they are located further apart, both in terms of the most abundant Operational Taxonomic Unit (OTU)s (PCA) and the least abundant (CA).

R1 showed very large differences in microbial community between the samples taken before and after the introduction of EA and the change in ORP conditions (Fig. 7). Some of the genera that decreased their abundance from P1 to P2 only in R1 (see Fig. 8) were *Trichococcus* (fermenter facultative anaerobe [63]), *Propioniciclav*a (fermenter facultative anaerobe [74]), CL500-29 marine group (aerobic heterotroph [10]), *Romboutsia* (strict anaerobic fermenter [24]), *Candidatus Sarcinitrix* (fermenter and aerobic heterotroph [58]), *Christensenellaceae* R-7 group (strict anaerobic fermenter [52]), and a number of not yet identified organisms: midas g 724, midas g 31, midas g 17, whose function

remains unknown.

On the other hand, the abundance of other organisms increased from P1 to P2 only in R1 (see Fig. 8). Interestingly, these organisms can perform denitrification; at least two are known to reduce  $\text{NO}_2^-$ . *Pseudomoxanthomonas* and *Luteimonas*'s abundance increased from 0 to 2.9 and 4.1 %, respectively. Both microorganisms are uncommon in activated sludge and were not present in the mixed liquor samples. *Pseudoxanthomonas* was mainly of the species *yeongjuensis* (1.7 %), which are known to be able to reduce nitrite but not nitrate [92], while *Luteimonas* has been shown capable of reducing nitrite to nitrous oxide, but not nitrate [11]. *Simplicispira* and *Hyphomicrobium*, two denitrifiers [68,84], also increased in abundance in R1, from 0.2 to 2.9 % and 0.6 to 3.4 %, respectively.

The abundance of nitrifying bacteria dramatically increased from P1 to P2 in both reactors (see Fig. 8,S6). While nitrifying bacteria represented, in total, 1.4 % of the organisms in the mixed liquor samples, the abundance in the biofilm samples increased from 0.2 to 6.7 % in R1 and 0.8 to 5.3 % in R2. The most abundant genus was *Nitrospira* (3.8 and 2.8 %). While two more nitrite oxidizers: *Nitrobacter* (1 and 0.2 %) and *Nitrotoga* (0.1 and 0.3 %), were present, the only known ammonia oxidizer found was *Nitrosomonas* (1.8 and 2 %).

Seven out of the 20 most abundant genera in the samples were known or suggested to grow by fermentation (see Fig. 8): *Tetrasphera*, *Ca. Amarolinea*, *Ca. Promineofilum*, *Ca. Competibacter*, *Trichococcus*, *Micropruina*, and *Rhodoferrax* [55,58,51,50,39,22]. Furthermore, it was

primarily organisms with this ability that have shown a decrease in abundance in both reactors from P1 to P2: *Ca. Promineofilum* decreased its abundance from 4.9 and 6.8 to 0.6 and 1.4 %, respectively, and *Micropruina* decreased from 1.1 and 4.1 to 0.4 and 1.5 %, respectively.

Regarding organisms with functions involved in sulfur and/or iron reduction/oxidation, such as sulfur-reducing bacteria (SRB), sulfur-oxidizing bacteria (SOB), and iron-reducing bacteria (IRB), the mixed liquor samples (MB0) contained a higher abundance of these organisms than biofilm samples (see Fig. S7). The highest abundances in MB0 corresponded to: *Dechloromonas* (3.5 %), *Rhodoferrax* (1.7 %), *Sulfuritalea* (0.8 %) and *Leptothrix* (0.6 %).

## 4. Discussion

### 4.1. ORP and N/Fe/S interactions

This section discusses the potential Fe and S interactions under anaerobic conditions and their detrimental effect on nitrification. When the MABRs were operating under the lowest ORP conditions (P1), NRs were low (Fig. 3), the ratio between OTR and NR was high (Fig. 3),  $\text{SO}_4^{2-}$  and  $\text{Fe}_{\text{dis}}$  compounds were being converted (Table 1), the membranes presented evidence of FeS precipitation (Fig. 5), and the abundance of nitrifying organisms in the biofilm was very low (Fig. 7, S6).

Sulfur conversions are complex and interrelated, including Fe/S interactions, because sulfur can be chemically and biologically transformed [71]. Under anaerobic conditions, SRB oxidize organics for cell growth and energy generation using oxidized sulfur compounds as electron acceptors ( $\text{SO}_4^{2-}$ ,  $\text{SO}_3^{2-}$ ,  $\text{S}^0$ ) [44]. SRB occurrence in anaerobic and even aerobic wastewater biofilms has been extensively reported [56,67,59], including MABRs [75]. Moreover, reduced inorganic sulfur compounds, such as  $\text{S}^0$  or ( $\text{H}_2\text{S}/\text{HS}^-$ ) can be used as electron donors for denitrification [66,86].

Iron compounds in the wastewater can also be reduced under anaerobic conditions to ferrous ions ( $\text{Fe}^{2+}$ ) [32]. The facility uses ferric salts ( $\text{FeSO}_4$ ) in the primary settler tanks to assist with phosphorus removal. A portion of these salts will precipitate with  $\text{PO}_4^{3-}$ , while the rest will combine with hydroxide ions to form HFO-Ps [26]. Under anaerobic conditions, HFO-Ps will be reduced, and the adsorbed phosphate will be released [34,86] found that iron reduction rates in sludge from a facility applying chemical  $\text{PO}_4^{3-}$  removal (like the one in this study) were as high as  $2.99 \text{ mg Fe g VSS}^{-1} \text{ h}^{-1}$ . The resulting reduced iron and sulfur compounds, sulfide ( $\text{H}_2\text{S}/\text{HS}^-$ ) and  $\text{Fe}^{2+}$  can precipitate to form FeS. Moreover, ferric phosphate can also oxidize  $\text{H}_2\text{S}/\text{HS}^-$  to form FeS, releasing  $\text{PO}_4^{3-}$  into the bulk [70].

In this study, using SEM-EDX and ICP-OES analysis, we found Fe:S molar ratios indicating the presence of FeS substances in the biofilm, such as pyrite or mackinawite, under the lowest ORP conditions (see Fig. 5, Fig. 6, Fig. S2, Fig. S3). Precipitation of inorganic components in the biofilm can lead to increased mass-transfer limitations, microbial displacement, clogging, poor flow distribution, and even fiber brittleness [31,48,21] and FeS precipitation in biofilms has been shown to decrease biofilm activity [37].

Results from the 16 s rRNA analysis show that the identified SRB, SOB, and IRB (to a lesser extent) were primarily present in mixed liquor samples but at higher relative abundances than commonly observed for average Danish WWTPs: *Rhodoferrax* 1.7 versus 0.7 % and *Dechloromonas* 3.5 versus 1.5 % [19] (see Fig. 8). The MABR tanks are continuously fed with anaerobic mixed liquor from an EBPR anaerobic zone at Ejby Mølle. Therefore, SRB and IRB are not expected to be significantly affected by the MABR's biofilm detachment or suspended growth inside the MABR tanks due to the low hydraulic retention time. Fig. 8 shows that the microbial community in the two suspended growth samples from R1 and R2 was almost identical. However, results from the two different periods of operation show that the activity of SRB and IRB present primarily in the mixed liquor can be mitigated by controlling the ORP levels in the tanks, in the case of the study, by introducing EA.

If dissolved oxygen is present, both  $\text{H}_2\text{S}/\text{HS}^-$  and  $\text{Fe}^{2+}$  may be oxidized either chemically or biologically. The oxidation of  $\text{H}_2\text{S}/\text{HS}^-$  requires oxygen in the range of  $0.5 \text{ g O}_2 (\text{g S})^{-1}$  to  $2 \text{ g O}_2 (\text{g S})^{-1}$  depending on the final product [54], while  $0.14 \text{ g O}_2 (\text{g Fe}^{2+})^{-1}$  is needed for the conversion of  $\text{Fe}^{2+}$  to ferric ion ( $\text{Fe}^{3+}$ ) and  $0.8 \text{ g O}_2 (\text{g FeS})^{-1}$  to re-oxidize FeS (precipitating  $\text{PO}_4^{3-}$ ) [23]. Internal sulfide re-oxidation can account for up to 70 % of oxygen consumption in aerobic biofilms [59]. Moreover, Sahinkaya et al., 2011 suggest that SOBs are better scavengers for low oxygen concentrations than aerobic heterotrophs. The ratio between NR and OTR during the P1 (lower ORP) was much higher than in P2 (higher ORP and cleaning/replacing membranes). This ratio decreased from 18 to 11 in R1 and 21 to 15 in R2 (see Table 2). Assuming the theoretical ratio of  $4.57 \text{ g O}_2 \text{ g N}^{-1}$  when oxygen is solely used to oxidize  $\text{NH}_x$  to  $\text{NO}_3^-$  [28], these results indicate the existence of other oxygen-demanding processes taking place in the biofilm for this particular scenario, which could be  $\text{H}_2\text{S}/\text{HS}^-$  and  $\text{Fe}^{2+}$  oxidation.

Besides the potential additional oxygen consumption,  $\text{H}_2\text{S}$  is produced chemically or by SRBs either in the mixed liquor or the outer layers of the MABR biofilms, and potentially upstream of the MABRs as well (primary settler or/and EBPR zones) when diffusing into the biofilm, could inhibit nitrifying activity. In this study, we could not accurately measure  $\text{H}_2\text{S}$  concentrations. However, the observed reduction in  $\text{SO}_4^{2-}$  indicates  $\text{H}_2\text{S}$  formation in the MABR reactors. Moreover,  $\text{H}_2\text{S}$  could be present in the MABR feed being produced upstream in the EBPR reactor, the primary settler, or the sewage system. The lack of stripping of volatile compounds is one of MABR's well-known characteristics [7], and it is generally acknowledged as a benefit. However, it could be detrimental in specific cases [73], such as this one.

[5] found that sulfide was a potent nitrification inhibitor and the maximum sulfide concentration the sludge could tolerate without affecting nitrification was  $1 \text{ mg S L}^{-1}$ ; it affected the nitrite oxidation step more than the ammonia oxidation step. [15] studied the resilience to sulfide inhibition in two samples from full-scale activated sludge treatment plants and found that sulfide had a substantial impact on nitrification, and the response was community-specific. The study also found that ammonia oxidizers were less vulnerable ( $K_i$  between 7.8 and  $14 \text{ mg S L}^{-1}$ ) than nitrite oxidizers (between 2.4 and  $6.7 \text{ mg S L}^{-1}$ ). Recently, [14] studied the complex elemental and microbial interactions in a nitrifying MABR fed with synthetic anaerobic effluent (ammonium and methane) at different sulfide concentrations and found that using sulfide as an electron donor promoted elevated nitrous oxide emissions and ammonium production through dissimilatory nitrite reduction to ammonium. [9] reported the impact of operational conditions on sulfur transformations and how this also impacted nitrogen and methane removal from reject water streams using membrane biofilm reactors.

This study shows that the complex interactions between N, Fe, and S compounds play a crucial role in MABR nitrification performance, particularly at low ORP. The low ORP conditions in P1 promoted the reduction of iron and sulfur compounds (either chemically or biologically), hindering nitrification performance mainly due to 1) precipitation of FeS acting as a coating agent and/or competing with biomass for space; 2) re-oxidation to  $\text{S}_0/\text{SO}_x$  and HFO which increases the internal oxygen demand; and, 3)  $\text{H}_2\text{S}$  inhibition of ammonia and nitrite-oxidizing organisms (see Table 1, Fig. 3 and Fig. 5). Moreover, under low ORP conditions, more  $\text{NH}_x$  is to be released from ammonification in the mixed liquor, reducing the overall nitrogen removal performance.

### 4.2. Combining nitrification and anaerobic/anoxic processes in MABR

The creation of different layers occupied by organisms with different functions in MABRs for nitrogen removal and how it differs from conventional biofilms have been extensively reported [91,78,38]. The different layers include (from the membrane base towards the bulk): nitrifying organisms, aerobic ordinary heterotrophic organisms, anoxic ordinary heterotrophic organisms (denitrifying organisms) or nitrifying



organisms, and anammox bacteria (if organic carbon is limited). Some of the first MABR studies, however, back when MABRs were called Permeable-Support Biofilms or Substratum-Aerated-Biofilm Reactor, hypothesized the existence of a fourth anaerobic layer, closer to the bulk, which would be beneficial to reduce solids production and provide readily available COD compounds to the inner biofilm [80]. Abdel-Warith et al. [11] confirmed the existence of this anaerobic layer when feeding the lab-scale reactor with high concentrations of acetate. This fourth anaerobic layer is generally omitted in the literature [7,60]; however, in this study, we found a high abundance of fermenting organisms in P1.

[33] tried to achieve concurrent COD and N removal with methane production by introducing MABRs into anaerobic reactors treating high-strength industrial wastewater. That study shows that the bioreactors improved COD removal but failed to remove nitrogen and maintain methane production. A more recent study focused on the coexistence of nitrification, denitrification, and sulfate reduction in MABRs, and operated the lab-scale reactor at low and high bulk dissolved oxygen concentrations, but not under anoxic or anaerobic conditions [45].

Sulfur-related processes in MABR had up until recently been primarily studied in membrane biofilm reactors fed with hydrogen, not MABRs. Terada et al., 2006 found in a membrane biofilm reactor fed with hydrogen gas that SRBs did not grow well while the ORP in the biofilm was high (0 mV), but they observed that 50 % of the sulfate was converted by SRBs when ORP was decreased to -300 mV. More recently, MABR has been identified as an efficient technology to recover sulfur via sulfide-oxidizing bacteria, as the counter-diffusional characteristics of the biofilm allow for more efficient oxygen control [75,27].

#### 4.3. Nitrification rates

Quantification of nitrification rates in full-scale hybrid MABRs can be challenging. The ratio between OTR, which can be more easily monitored, and NR, could be used to calculate NR based on OTR values and the stoichiometric ratio of  $4.57 \text{ g O}_2 \text{ g N}^{-1}$ . This would only be representative if most of the oxygen were used to convert  $\text{NH}_x$  to  $\text{NO}_3$ . If partial nitrification happened instead, this ratio would be lower, and NR would be underestimated. If other oxygen-consuming processes were taking place, as in this study, NR could be overestimated. This study observed OTR/NR close to 20 during P1, almost four times higher than the theoretical 4.57. Estimating NR using this method would have led to a considerable overestimation of NR.

Biomass assimilation and ammonia release should also be considered to quantify NR accurately. Mass balancing over measurements other than  $\text{NH}_x$ , such as TN, would help better understand the system. In this study, however, due to the high MLSS concentrations and the inaccuracies associated with it, TN measurements could not be used. Due to the anaerobic conditions of the reactors in P1 and the high MLSS, the authors hypothesize that  $\text{NH}_x$  release could have been significant in this study, increasing the reported NR. However, it was not possible to quantify its contribution.

Although the improvements in NR observed in P2 in this study are still lower than previously reported for full-scale hybrid MABRs. Average values of NR of  $2.1 \text{ g N m}^{-2} \text{ d}^{-1}$  [25] and  $3.7 \text{ g N m}^{-2} \text{ d}^{-1}$  [69] have been recently reported in full-scale hybrid MABR experiences. This could be partially caused by the uncertainty in what was the exact NR occurring in the system, as previously discussed, but it could also have other potential causes. As discussed in [81], this study shows the highest MLSS ever reported for a hybrid MABR. At these high MLSS concentrations, a less-than-optimal mixing of the MABR reactors could have had a negative impact. Hydrodynamics can have a significant effect on biofilm activity. Indeed, [69] observed the highest NR when mixing was increased. In this study, R2 obtained the highest NR when the mixing was increased (P2b) and R1 when EA was the highest (P2). Adequate mixing of full-scale MABRs and its potential impact on NR should be further investigated.

#### 4.4. Phosphate removal

The results reported in Table 1 provide evidence that MABR surprisingly impacted phosphate removal at the reactors, and this remained unaffected by the changes in ORP conditions. In both P1 and P2, contrary to expectations for an anaerobic reactor, the average  $\text{PO}_4^{3-}$  removal efficiency was 50 and 57 % (Table 1). Phosphate removal in the MABRs could take place chemically and/or biologically. Some of the existing mechanisms could be: a) a fraction of the  $\text{PO}_4^{3-}$  could precipitate in the biofilm with the Ca present in the wastewater [35]; b)  $\text{Fe}^{2+}$  could precipitate phosphate (e.g., vivianite) [90] and its oxidation product  $\text{Fe}^{3+}$  could also precipitate phosphate or adsorb phosphate in the form of HFO [26]; and c)  $\text{PO}_4^{3-}$  could be converted biologically by denitrifying polyphosphate-accumulating organisms (DPAO) activity [41].

The biological conversion of  $\text{PO}_4^{3-}$  is carried out by polyphosphate-accumulating organisms (PAOs) using  $\text{O}_2$  or by DPAOs using  $\text{NO}_x$  as electron acceptor and it could be taking place in either the biofilm or the suspended growth fraction of the reactors. The MABRs are fed with anaerobic mixed liquor from an EBPR zone, and 16 s rRNA analysis confirms the presence of PAOs (see Fig. 8) in both the mixed liquor and the MABR biofilm. In the first option, PAOs (including DPAOs) present in the mixed liquor, which have been through an anaerobic zone containing volatile fatty acids, would take up the  $\text{PO}_4^{3-}$  in the wastewater using either  $\text{O}_2$  or  $\text{NO}_x$ . The low ORP conditions in both R1 and R2, even during P2, suggest that dissolved oxygen was not present in the mixed liquor (confirmed by spot measurements), and  $\text{NO}_2^-$  or  $\text{NO}_3^-$  was most likely the electron acceptor used by DPAOs. This is in line with previous studies carried out at this facility, which showed that a very high fraction of the PAO community was able to utilize  $\text{NO}_2^-$  or  $\text{NO}_3^-$  [82].

However, analysis of the biofilms also showed a high abundance of PAOs (*Tetrasphaera*, *Dechloromonas*), with *Tetrasphaera* as the most abundant genus in most samples (see Fig. 8). Biological phosphorus removal could occur in the biofilm if transient anaerobic/anoxic or anaerobic/oxic conditions were taking place, as typically happens in sequencing batch reactors [85] or granular sludge [13,76] used an MABR in a sequencing batch reactor combined with intermittent aeration and achieved 85 % total phosphorus removal. The modeling study carried out by [6] also reported higher P removal efficiencies when comparing an MABR with a traditional A2O configuration due to the denitrifying effect of PAOs. Biofilm attachment of *Tetrasphaera* organisms present in the mixed liquor could also be partly responsible for its high abundance in the biofilm, as biofilm attachment plays a key role in biofilm function [36]. The mechanisms behind phosphorus removal in this study are unclear and are currently under investigation.

#### 4.5. Lessons learned

The implementation of EA (R1, R2) increased ORP conditions by oxidizing and stripping reduced compounds, such as  $\text{H}_2\text{S}/\text{HS}^-$  and  $\text{Fe}_{\text{dis}}$ , and did not allow the growth of either SRB and IRB or the chemical S and Fe transformations, which caused the above-mentioned problems (precipitation, oxygen consumption and/or inhibition) (P2). Values in Table 1 showed reduced  $\text{SO}_4^{2-}$  and  $\text{Fe}_{\text{dis}}$  conversion and higher ammonia conversion rates in P2 than in P1. The contribution of nitrification to the overall oxygen transfer across the membranes increased significantly from P1 to P2 (see Fig. 3 and Table 2), as the relative abundance of nitrifiers in the biofilm also increased (see Fig. 8 and Fig. S9).

Replacing and chemically cleaning the membranes had different chemical and microbial composition effects. Replacing the membranes (R1) while implementing EA proved helpful in growing a different microbial community in the biofilm (Fig. 7), since the new biofilm started to develop in a new, less reduced environment. The chemical compositional analysis showed that FeS was present in a sample from R1 in P1 but not from P2. However, inorganic iron and calcium phosphate minerals mainly remained unchanged.

Chemical cleaning of the membranes (R2) was successful in

removing all inorganic precipitates from the membranes, including iron (Fig. 5). After approximately-eight months of operation in R2, the microbial community of the biofilm in P2 was more similar to that in P1, and also to that of the suspended growth fraction (Fig. 7). [79] found significant shifts in the microbial community under changing operating conditions in a lab-scale MABR. However, results from this study suggest that the initial biofilm formation might have played a more important role in overall microbial community structure than changing operating conditions, but more work would be necessary to confirm this.

Literature suggests that the best location for MABRs to remove N, COD, and P, using the least resources, is in a bioreactor preceded by anaerobic zones (if bio-P is desired) and followed by a “polishing” aerobic reactor [6]. In this configuration, denitrification occurs in the MABR zones without a recirculation stream from an aerobic zone. To avoid the detrimental effects of low ORP reported in this study, MABRs should be carefully designed when preceded by anaerobic zones (without recirculation stream from aerobic zones) treating wastewater containing Fe and S compounds. Some potential solutions to circumvent the problem could be adding a small aerobic zone prior to the MABR, similar to the EA in this study, which has been shown to improve the performance significantly or increasing the fraction of MABR volume versus suspended growth volume, which would decrease the anaerobic retention time and increase the ORP levels. In this study, the MABR fraction of the total reactor volume was approximately 50 % for R1 and 25 % for R2.

Further work will be required to corroborate some of the mechanisms suggested in this study. Microbial and elemental interactions in environmental engineered systems are complex and intertwined. Controlled experiments at a smaller scale than the one used in this study would allow for a more robust understanding of the complex processes at place.

## 5. Conclusions

- Two hybrid MABRs with different membrane compositions were operated for over 1000 days and fed with anaerobic mixed liquor from an existing EBPR zone. The study was further divided into P1 and P2, i.e., before and after introducing fine bubble aeration in the reactors, and membranes were either replaced (R1) or chemically cleaned (R2) between the two periods.
- P1 was characterized by low ORP in both reactors ( $-370$  mV), low nitrification rates ( $0.3 \text{ g N m}^{-2} \text{ d}^{-1}$ ), while in P2, the introduction of fine bubble aeration brought ORP up to an average value of about  $-200$  mV, and the nitrification rates increased closer to  $1 \text{ g N m}^{-2} \text{ d}^{-1}$ .
- Chemical analysis of influent and effluent suggests a concurrent reduction of  $\text{SO}_4^{2-}$  and  $\text{Fe}_{\text{dis}}$  was taking place in the reactors in P1, and it decreased (or did not happen) in P2.  $\text{NH}_x$  removal increased from 21 % to 35 %.
- Both  $\text{NO}_2^-$  and  $\text{NO}_3^-$  in the effluent remained low during the whole study period (average of  $0.0$  and  $0.5 \text{ g N m}^{-3}$ , respectively) and  $\text{PO}_4^{3-}$  removal rates were similar in P1 and P2, with averages of 50 and 57 %.
- Elemental composition analysis of the biofilm using SEM-EDX showed an accumulation of inorganic precipitates during both periods. Samples from P1 showed presence of Fe and S, which disappeared in P2. Chemical cleaning in R2 successfully removed all inorganic precipitates, including the highly abundant Fe, Ca, and P.
- Microbial analysis using 16 s rRNA amplicon sequencing showed that R1 had a significantly different microbial community for the two periods compared with R2, which showed a more similar microbial community in both periods that was also very close to the microbial community composition of mixed liquor samples.
- The biofilms showed a high abundance of heterotrophic organisms and organisms with fermenting capabilities (*Tetrasphaera* being the most abundant), which significantly decreased from P1 to P2. On the

other hand, the abundance of nitrifying organisms in the biofilm samples from both reactors dramatically increased from P1 to P2, when they were approximately-five times more abundant than in the mixed liquor samples. SRB, SOB, and IRB organisms were present mainly in the mixed liquor samples.

## Declaration of Competing Interest

The authors declare that they have no known competing financial interests or personal relationships that could have appeared to influence the work reported in this paper.

## Data availability

Data will be made available on request.

## Acknowledgments

Nerea Uri-Carreño gratefully acknowledges the Industrial Ph.D. program's financial support from Innovation Fund Denmark, through the project “MANTRA” (Contract-No: 7091-00038A). Dr. Xavier Flores-Alsina and Prof. Krist Gernaey also thank the Danish Council for Independent Research in the frame of the DFF FTP research project GREENLOGIC (Contract-No:7017-00175A) and the Danida fellowship center (DFC) research project ERASE (Contract-No: 18-M09-DTU). Professor Ulla Gro Nielsen and Dr. Qian Wang thank The Danish Research Council - Technology and Production Science grant (Contract-No: 7017-00262).

## Appendix A. Supplementary data

Supplementary data to this article can be found online at <https://doi.org/10.1016/j.cej.2022.138917>.

## References

- [1] A.S. Abdel-Warith, K.J. Williamson, S.E. Strand, 1990. Substratum-Aerated-Biofilm Reactor. Proc. 1990 Spec. Conf. Environ. Eng.
- [2] V. Acevedo Alonso, S. Lackner, Membrane aerated biofilm reactors – how longitudinal gradients influence nitrogen removal – a conceptual study, Water Res. 166 (2019), 115060, <https://doi.org/10.1016/j.watres.2019.115060>.
- [4] K.S. Andersen, R.H. Kirkegaard, S.M. Karst, M. Albertsen, ampvis2: an R package to analyse and visualise 16S rRNA amplicon data, Biorxiv (2018), <https://doi.org/10.1101/299537>.
- [5] D.I. Bejarano-Ortiz, S. Huerta-Ochoa, F. Thalasso, F. de María Cuervo-López, A. C. Texier, Kinetic constants for biological ammonium and nitrite oxidation processes under sulfide inhibition, Appl. Biochem. Biotechnol. 177 (2015) 1665–1675, <https://doi.org/10.1007/s12010-015-1844-3>.
- [6] A.L. Carlson, H. He, C. Yang, G.T. Daigger, Comparison of hybrid membrane aerated biofilm reactor (MABR)/suspended growth and conventional biological nutrient removal processes, Water Sci. Technol. 83 (2021) 1418–1428, <https://doi.org/10.2166/wst.2021.062>.
- [7] E. Casey, B. Glennon, G. Hamer, Review of membrane aerated biofilm reactors, Resour. Conserv. Recycl. 27 (1999) 203–215, [https://doi.org/10.1016/S0921-3449\(99\)00007-5](https://doi.org/10.1016/S0921-3449(99)00007-5).
- [8] M. Castrillo, R. Díez-Montero, A.L. Esteban-García, I. Tejero, Mass transfer enhancement and improved nitrification in MABR through specific membrane configuration, Water Res. 152 (2019) 1–11, <https://doi.org/10.1016/j.watres.2019.01.001>.
- [9] X. Chen, Y. Liu, L. Peng, Z. Yuan, B.J. Ni, Model-based feasibility assessment of membrane biofilm reactor to achieve simultaneous ammonium, dissolved methane, and sulfide removal from anaerobic digestion liquor, Sci. Rep. 6 (2016) 1–13, <https://doi.org/10.1038/srep25114>.
- [10] Z.J. Chen, C.Y. Ding, J.Y. Zhu, L.I. Bing, H. Jin, D.U. Zong-Ming, Community structure and influencing factors of bacterioplankton during low water periods in danjiangkou reservoir, China Environ. Sci. 37 (2017) 336–344.
- [11] J. Cheng, M.-Y. Zhang, W.-X. Wang, D. Manikprabhu, N. Salam, T.-Y. Zhang, Y.-Y. Wu, W.-J. Li, Y.-X. Zhang, Luteimonas notoginsengisoli sp. nov., isolated from rhizosphere, Int. J. Syst. Evol. Microbiol. 66 (2016) 946–950, <https://doi.org/10.1099/ijsem.0.000816>.
- [12] S.F. Corsino, M. Torregrossa, Achieving complete nitrification below the washout SRT with hybrid membrane aerated biofilm reactor (MABR) treating municipal wastewater, J. Environ. Chem. Eng. 10 (2022), 106983, <https://doi.org/10.1016/j.cej.2021.106983>.



- [13] D.R. de Graaff, M.C.M. van Loosdrecht, M. Pronk, Biological phosphorus removal in seawater-adapted aerobic granular sludge, *Water Res.* 172 (2020), <https://doi.org/10.1016/j.watres.2020.115531>.
- [14] J. Delgado Vela, L.A. Bristow, H.K. Marchant, N.G. Love, G.J. Dick, Sulfide alters microbial functional potential in a methane and nitrogen cycling biofilm reactor, *Environ. Microbiol.* 23 (2021) 1481–1495, <https://doi.org/10.1111/1462-2920.15352>.
- [15] J. Delgado Vela, G.J. Dick, N.G. Love, Sulfide inhibition of nitrite oxidation in activated sludge depends on microbial community composition, *Water Res.* 138 (2018) 241–249, <https://doi.org/10.1016/j.watres.2018.03.047>.
- [16] L.S. Downing, R. Nerenberg, Total nitrogen removal in a hybrid, membrane-aerated activated sludge process, *Water Res.* 42 (2008) 3697–3708, <https://doi.org/10.1016/j.watres.2008.06.006>.
- [17] M.S. Dueholm, K.S. Andersen, S.J. McIlroy, J.M. Kristensen, E. Yashiro, S.M. Karst, M. Albertsen, P.H. Nielsen, Generation of comprehensive ecosystem-specific reference databases with species-level resolution by high-throughput full-length 16S rRNA gene sequencing and automated taxonomy assignment (Autotax), *MBio* 11 (2020) 1–14, <https://doi.org/10.1128/mBio.01557-20>.
- [18] M.S. Dueholm, M. Nierychlo, K.S. Andersen, V. Rudkjøbing, S. Knudsen, the MiDAS Global Consortium, M. Albertsen, P.H. Nielsen, 2021. MiDAS 4: A global catalogue of full-length 16S rRNA gene sequences and taxonomy for studies of bacterial communities in wastewater treatment plants. *BioRxiv*.
- [19] A. Elsayed, M. Hurdle, Y. Kim, Comprehensive model applications for better understanding of pilot-scale membrane-aerated biofilm reactor performance, *J. Water Process Eng.* 40 (2021), 101894, <https://doi.org/10.1016/j.jwpe.2020.101894>.
- [20] H. Feldman, X. Flores-Alsina, P. Ramin, K. Kjellberg, U. Jeppsson, D.J. Batstone, K. V. Gernaey, Assessing the effects of intra-granule precipitation in a full-scale industrial anaerobic digester, *Water Sci. Technol.* 79 (2019) 1327–1337, <https://doi.org/10.2166/wst.2019.129>.
- [21] K.T. Finneran, C.V. Johnson, D.R. Lovley, *Rhodospirillum rubrum* sp. nov., a psychrotolerant, facultatively anaerobic bacterium that oxidizes acetate with the reduction of Fe(III), *Int. J. Syst. Evol. Microbiol.* 53 (2003) 669–673, <https://doi.org/10.1099/ijs.0.02298-0>.
- [22] H. Ge, L. Zhang, D.J. Batstone, J. Keller, Z. Yuan, Impact of iron salt dosage to sewers on downstream anaerobic sludge digesters: sulfide control and methane production, *J. Environ. Eng.* 139 (2013) 594–601, [https://doi.org/10.1061/\(asce\)ee.1943-7870.0000650](https://doi.org/10.1061/(asce)ee.1943-7870.0000650).
- [23] J. Gerritsen, S. Fuentes, V. Grievink, L. van Niftrik, B.J. Tindall, H.M. Timmerman, G.T. Rijkers, H. Smidt, Characterization of *Romboutsia ilealis* gen. nov., sp. nov., isolated from the gastro-intestinal tract of a rat, and proposal for the reclassification of five closely related members of the genus *Clostridium* into the genera *Romboutsia* gen. nov., *Intestini*. *Int. J. Syst. Evol. Microbiol.* 64 (2014) 1600–1616, <https://doi.org/10.1099/ijs.0.059543-0>.
- [24] G. Guglielmi, D. Coutts, D. Houweling, J. Peeters, Full-scale application of mabr technology for upgrading and retrofitting an existing WWTP: Performances and process modelling, *Environ. Eng. Manag. J.* 19 (2020) 1781–1789, <https://doi.org/10.30638/eemj.2020.169>.
- [25] H. Hauduc, I. Takács, S. Smith, A. Szabo, S. Murthy, G.T. Daigger, M. Spérandio, A dynamic physicochemical model for chemical phosphorus removal, *Water Res.* 73 (2015) 157–170, <https://doi.org/10.1016/j.watres.2014.12.053>.
- [26] H. He, B.M. Wagner, A.L. Carlson, C. Yang, G.T. Daigger, Recent progress using membrane aerated biofilm reactors for wastewater treatment, *Water Sci. Technol.* 00 (2021) 1–27, <https://doi.org/10.2166/wst.2021.443>.
- [27] M. Henze, P. Harremoës, J. la Cour Jansen, E. Arvin, Wastewater treatment - Biological and chemical processes, *Environ. Eng.* (2002), <https://doi.org/10.1007/978-3-662-22605-6>.
- [28] D. Houweling, G.T. Daigger, Intensifying activated sludge using media-supported biofilms, 1st Editio. ed., CRC Press, 2019.
- [29] D. Houweling, Z. Long, J. Peeters, N. Adams, P. Côté, G. Daigger, S. Snowling, Nitrifying below the “washout” SRT: Experimental and modelling results for a hybrid MABR/activated sludge process. 91st Annu. Water Environ. Fed. Tech. Exhib. Conf. WEFTEC (2019) 1250–1270, <https://doi.org/10.2175/193864718825137944>.
- [30] J.H. Hwang, N. Cicek, J.A. Oleszkiewicz, Long-term operation of membrane biofilm reactors for nitrogen removal with autotrophic bacteria, *Water Sci. Technol.* 60 (2009) 2405–2412, <https://doi.org/10.2166/wst.2009.624>.
- [31] P. Jameel, The use of ferrous chloride to control dissolved sulfides in interceptor sewers, *J. Water Pollut. Control Fed.* 61 (1989) 230–236.
- [32] A.S. Kappell, M.J. Semmens, P.J. Novak, T.M. Lapara, Novel application of oxygen-transferring membranes to improve anaerobic wastewater treatment, *Biotechnol. Bioeng.* 89 (2005) 373–380, <https://doi.org/10.1002/bit.20219>.
- [33] C. Kazadi Mbamba, E.U. Lindblom, X. Flores-Alsina, S. Tait, S. Anderson, R. Saagi, D.J. Batstone, K.V. Gernaey, U. Jeppsson, Plant-wide model-based analysis of iron dosing strategies for chemical phosphorus removal in wastewater treatment systems, *Water Res.* 155 (2019) 12–25, <https://doi.org/10.1016/j.watres.2019.01.048>.
- [34] C. Kazadi Mbamba, S. Tait, X. Flores-Alsina, D.J. Batstone, A systematic study of multiple minerals precipitation modelling in wastewater treatment, *Water Res.* 85 (2015) 359–370, <https://doi.org/10.1016/j.watres.2015.08.041>.
- [35] M.M.T. Khan, T. Chapman, K. Cochran, A.J. Schuler, Attachment surface energy effects on nitrification and estrogen removal rates by biofilms for improved wastewater treatment, *Water Res.* 47 (2013) 2190–2198, <https://doi.org/10.1016/j.watres.2013.01.036>.
- [36] B. Kiellerich, P. Kiellerich, A.H. Nielsen, J. Vollertsen, Variations in activities of sewer biofilms due to ferrous and ferric iron dosing, *Water Sci. Technol.* 2017 (2018) 845–858, <https://doi.org/10.2166/wst.2018.261>.
- [37] C.T. Kinh, S. Riya, M. Hosomi, A. Terada, Identification of hotspots for NO and N<sub>2</sub>O production and consumption in counter- and co-diffusion biofilms for simultaneous nitrification and denitrification, *Bioresour. Technol.* 245 (2017) 318–324, <https://doi.org/10.1016/j.biortech.2017.08.051>.
- [38] Y.H. Kong, M. Beer, R.J. Seviour, K.C. Lindrea, G.N. Rees, Structure and functional analysis of the microbial community in an aerobic: anaerobic sequencing batch reactor (SBR) with no phosphorus removal, *Syst. Appl. Microbiol.* 24 (2001) 597–609, <https://doi.org/10.1078/0723-2020-00075>.
- [39] D.J. Lane, 16S/23S rRNA Sequencing, in: E. Stackebrandt, M. Goodfellow (Eds.), *Nucleic Acid Techniques in Bacterial Systematics*, John Wiley and Sons, New York, 1991, pp. 115–175.
- [40] A.B. Lanham, A. Oehmen, G. Carvalho, A.M. Saunders, P.H. Nielsen, M.A.M. Reis, Denitrification activity of polyphosphate accumulating organisms (PAOs) in full-scale wastewater treatment plants, *Water Sci. Technol.* 78 (2018) 2449–2458, <https://doi.org/10.2166/wst.2018.517>.
- [41] H. Li, Minimap2: pairwise alignment for nucleotide sequences, *Arxiv*, 2017.
- [42] H. Li, B. Handsaker, A. Wysoker, T. Fennell, J. Ruan, N. Homer, G. Marth, G. Abecasis, R. Durbin, The sequence alignment/map format and SAMtools, *Bioinformatics* 25 (2009) 2078–2079, <https://doi.org/10.1093/bioinformatics/btp352>.
- [43] S. Lin, H.R. Mackey, T. Hao, G. Guo, M.C.M. van Loosdrecht, G. Chen, Biological sulfur oxidation in wastewater treatment: a review of emerging opportunities, *Water Res.* 143 (2018) 399–415, <https://doi.org/10.1016/j.watres.2018.06.051>.
- [44] H. Liu, S. Tan, Z. Sheng, T. Yu, Y. Liu, Impact of oxygen on the coexistence of nitrification, denitrification, and sulfate reduction in oxygen-based membrane aerated biofilm, *Can. J. Microbiol.* 61 (2015) 237–242, <https://doi.org/10.1139/cjm-2014-0574>.
- [45] Y. Liu, Z. Zhang, N. Bhandari, Z. Dai, F. Yan, G. Ruan, A.Y. Lu, G. Deng, F. Zhang, H. Al-Saari, A.T. Kan, M.B. Tomson, New approach to study iron sulfide precipitation kinetics, solubility, and phase transformation, *Ind. Eng. Chem. Res.* 56 (2017) 9016–9027, <https://doi.org/10.1021/acs.iecr.7b01615>.
- [46] Y. Ma, A. Pisco, A.D.L.C. Veras, C. Domingo-Félez, B.F. Smets, Intermittent aeration to regulate microbial activities in membrane-aerated biofilm reactors: Energy-efficient nitrogen removal and low nitrous oxide emission, *Chem. Eng. J.* 133630 (2021), <https://doi.org/10.1016/j.cej.2021.133630>.
- [47] K.J. Martin, R. Nerenberg, The membrane biofilm reactor (MBfR) for water and wastewater treatment: Principles, applications, and recent developments, *Bioresour. Technol.* 122 (2012) 83–94, <https://doi.org/10.1016/j.biortech.2012.02.110>.
- [48] M. Martin, Cutadapt removes adapter sequences from high-throughput sequencing reads. *EMBnet.journal*; Vol 17, No 1 Next Gener. Seq. Data Anal. (2011), <https://doi.org/10.14806/eg.17.1.200>.
- [49] S.J. McIlroy, M. Albertsen, E.K. Andresen, A.M. Saunders, R. Kristiansen, M. Stokholm-Bjerregaard, K.L. Nielsen, P.H. Nielsen, ‘Candidatus Competibacter’-lineage genomes retrieved from metagenomes reveal functional metabolic diversity, *ISME J.* 8 (2014) 613–624, <https://doi.org/10.1038/ismej.2013.162>.
- [50] S.J. McIlroy, S.M. Karst, M. Nierychlo, M.S. Dueholm, M. Albertsen, R. H. Kirkegaard, R.J. Seviour, P.H. Nielsen, Genomic and in situ investigations of the novel uncultured chloroflexi associated with 0092 morphotype filamentous bulking in activated sludge, *ISME J.* 10 (2016) 2223–2234, <https://doi.org/10.1038/ismej.2016.14>.
- [51] M. Morotomi, F. Nagai, Y. Watanabe, Description of *Christensenella minuta* gen. nov., sp. nov., isolated from human faeces, which forms a distinct branch in the order Clostridiales, and proposal of *Christensenellaceae* fam. nov., *Int. J. Syst. Evol. Microbiol.* 62 (2012) 144–149, <https://doi.org/10.1099/ijs.0.026989-0>.
- [52] G. Muyzer, E.C. de Waal, A.G. Uitterlinden, Profiling of complex microbial populations by denaturing gradient gel electrophoresis analysis of polymerase chain reaction-amplified genes coding for 16S rRNA, *Appl. Environ. Microbiol.* 59 (1993) 695–700, <https://doi.org/10.1128/aem.59.3.695-700.1993>.
- [53] A.H. Nielsen, J. Vollertsen, T. Hvitved-Jacobsen, Kinetics and Stoichiometry of Aerobic Sulfide Oxidation in Wastewater from Sewers-Effects of pH and Temperature, *Water Environ. Res.* 78 (2006) 275–283, <https://doi.org/10.2175/106143005x94367>.
- [54] J.L. Nielsen, H. Nguyen, R.L. Meyer, P.H. Nielsen, Identification of glucose-fermenting bacteria in a full-scale enhanced biological phosphorus removal plant by stable isotope probing, *Microbiology* 158 (2012) 1818–1825, <https://doi.org/10.1099/mic.0.058818-0>.
- [55] P.H. Nielsen, W. Lee, Z. Lewandowski, M. Morison, W.G. Characklis, Corrosion of mild steel in an alternating oxic and anoxic biofilm system, *Biofouling* 7 (1993) 267–284, <https://doi.org/10.1080/08927019309386259>.
- [56] M. Nierychlo, K.S. Andersen, Y. Xu, N. Green, C. Jiang, M. Albertsen, M. S. Dueholm, P.H. Nielsen, MiDAS 3: An ecosystem-specific reference database, taxonomy and knowledge platform for activated sludge and anaerobic digesters reveals species-level microbiome composition of activated sludge, *Water Res.* 182 (2020), 115955, <https://doi.org/10.1016/j.watres.2020.115955>.
- [57] M. Nierychlo, A. Milobedzka, F. Petriglieri, B. McIlroy, P.H. Nielsen, S.J. McIlroy, The morphology and metabolic potential of the chloroflexi in full-scale activated sludge wastewater treatment plants, *FEMS Microbiol. Ecol.* 95 (2019), <https://doi.org/10.1093/femsec/fiy228>.
- [58] S. Okabe, T. Itoh, H. Satoh, Y. Watanabe, Analyses of spatial distributions of sulfate-reducing bacteria and their activity in aerobic wastewater biofilms, *Appl. Environ. Microbiol.* 65 (1999) 5107–5116, <https://doi.org/10.1128/aem.65.11.5107-5116.1999>.

- [60] C. Pellicer-Nàcher, C. Domingo-Félez, S. Lackner, B.F. Smets, Microbial activity catalyzes oxygen transfer in membrane-aerated nitrifying biofilm reactors, *J. Memb. Sci.* 446 (2013) 465–471, <https://doi.org/10.1016/j.memsci.2013.06.063>.
- [61] P. Perez-Calleja, M. Aybar, C. Picioreanu, A.L. Esteban-Garcia, K.J. Martin, R. Nerenberg, Periodic venting of MABR lumen allows high removal rates and high gas-transfer efficiencies, *Water Res.* 121 (2017) 349–360, <https://doi.org/10.1016/j.watres.2017.05.042>.
- [62] P. Pérez-Calleja, E. Clements, R. Nerenberg, Enhancing ammonium oxidation fluxes and nitrification efficiencies in MABRs: a modeling study, *Environ. Sci. Water Res. Technol.* 8 (2022) 358–374, <https://doi.org/10.1039/D1EW00337B>.
- [63] E.V. Pikuta, R.B. Hoover, A.K. Bej, D. Marsic, W.B. Whitman, P.E. Krader, J. Tang, *Trichococcus patagoniensis* sp. nov., a facultative anaerobe that grows at -5 degrees C, isolated from penguin guano in Chilean Patagonia, *Int. J. Syst. Evol. Microbiol.* 56 (2006) 2055–2062, <https://doi.org/10.1099/ijs.0.64225-0>.
- [64] R Core Team, 2020. R: A language and environment for statistical computing. R Foundation for Statistical Computing, Vienna, Austria.
- [65] RStudio Team, 2020. RStudio: Integrated Development Environment for R.
- [66] F. Sabba, A. DeVries, M. Vera, G. Druschel, C. Bott, R. Nerenberg, Potential use of sulfite as a supplemental electron donor for wastewater denitrification, *Rev. Environ. Sci. Biotechnol.* 15 (2016) 563–572, <https://doi.org/10.1007/s11157-016-9413-y>.
- [67] C.M. Santegeods, T.G. Ferdman, G. Muyzer, B. De Dirk, Structural and functional dynamics of sulfate-reducing populations in bacterial biofilms, *Appl. Environ. Microbiol.* 64 (1998) 3731–3739.
- [68] M.Z. Siddiqi, W. Sok, G. Choi, S.Y. Kim, J.-H. Wee, W.T. Im, *Simplicispira hankyongi* sp. nov., a novel denitrifying bacterium isolated from sludge, *Antonie Van Leeuwenhoek* 113 (2020) 331–338, <https://doi.org/10.1007/s10482-019-01341-0>.
- [69] I.T. Silveira, K. Cadee, W. Bagg, Startup and initial operation of an MLE-MABR treating municipal wastewater, *Water Sci. Technol.* 85 (2022) 1155–1166, <https://doi.org/10.2166/wst.2022.045>.
- [70] P.C. Singer, Anaerobic Control of Phosphate by Ferrous Iron. *J. (Water Pollut. Control Fed.* 44 (1972) 663–669.
- [71] K. Solon, X. Flores-Alsina, C. Kazadi Mbamba, D. Ikumi, E.I.P. Volcke, C. Vaneckhaute, G. Ekama, P.A. Vanrolleghem, D.J. Batstone, K.V. Gernaey, U. Jeppsson, Plant-wide modelling of phosphorus transformations in wastewater treatment systems: Impacts of control and operational strategies, *Water Res.* 113 (2017) 97–110, <https://doi.org/10.1016/j.watres.2017.02.007>.
- [72] M. Stokholm-Bjerregaard, S.J. McIlroy, M. Nierychlo, S.M. Karst, M. Albertsen, P. H. Nielsen, A Critical Assessment of the Microorganisms Proposed to be Important to Enhanced Biological Phosphorus Removal in Full-Scale Wastewater Treatment Systems, *Front. Microbiol.* 8 (2017) 718, <https://doi.org/10.3389/fmicb.2017.00718>.
- [73] A.-E. Stricker, H. Lossing, J.H. Gibson, Y. Hong, J.C. Urbanic, Pilot Scale Testing of A New Configuration of The Membrane Aerated Biofilm Reactor (MABR) to Treat High-Strength Industrial Sewage, *Water Environ. Res.* 83 (2011) 3–14, <https://doi.org/10.2175/106143009x12487095236991>.
- [74] Y. Sugawara, A. Ueki, K. Abe, N. Kaku, K. Watanabe, K. Ueki, *Propioniciclavida tarda* gen. nov., sp. nov., isolated from a methanogenic reactor treating waste from cattle farms, *Int. J. Syst. Evol. Microbiol.* 61 (2011) 2298–2303, <https://doi.org/10.1099/ijs.0.027482-0>.
- [75] J. Sun, X. Dai, Y. Liu, L. Peng, B.-J. Ni, Sulfide removal and sulfur production in a membrane aerated biofilm reactor: Model evaluation, *Chem. Eng. J.* 309 (2017) 454–462, <https://doi.org/10.1016/j.cej.2016.09.146>.
- [76] L. Sun, Z. Wang, X. Wei, P. Li, H. Zhang, M. Li, B. Li, S. Wang, Enhanced biological nitrogen and phosphorus removal using sequencing batch membrane-aerated biofilm reactor, *Chem. Eng. Sci.* 135 (2015) 559–565, <https://doi.org/10.1016/j.ces.2015.07.033>.
- [77] E. Syron, M.J. Semmens, E. Casey, Performance analysis of a pilot-scale membrane aerated biofilm reactor for the treatment of landfill leachate, *Chem. Eng. J.* 273 (2015) 120–129, <https://doi.org/10.1016/j.cej.2015.03.043>.
- [78] A. Terada, K. Hibiya, J. Nagai, S. Tsuneda, A. Hirata, Nitrogen removal characteristics and biofilm analysis of a membrane-aerated biofilm reactor applicable to high-strength nitrogenous wastewater treatment, *J. Biosci. Bioeng.* 95 (2003) 170–178, <https://doi.org/10.1263/jbb.95.170>.
- [79] H.L. Tian, J.Y. Zhao, H.Y. Zhang, C.Q. Chi, B.A. Li, X.L. Wu, Bacterial community shift along with the changes in operational conditions in a membrane-aerated biofilm reactor, *Appl. Microbiol. Biotechnol.* 99 (2015) 3279–3290, <https://doi.org/10.1007/s00253-014-6204-7>.
- [80] D.L. Timberlake, S.E. Strand, K.J. Williamson, Combined aerobic heterotrophic oxidation, nitrification and denitrification in a permeable-support biofilm, *Water Res.* 22 (1988) 1513–1517, [https://doi.org/10.1016/0043-1354\(88\)90163-7](https://doi.org/10.1016/0043-1354(88)90163-7).
- [81] N. Uri-Carreño, P.H. Nielsen, K.V. Gernaey, X. Flores-Alsina, Long-term operation assessment of a full-scale membrane-aerated biofilm reactor under Nordic conditions, *Sci. Total Environ.* 779 (2021), 146366, <https://doi.org/10.1016/j.scitotenv.2021.146366>.
- [82] N. Uri Carreño, P. Nielsen, T. Constantine, K. Chandran, C. Hoar, C. De Barbaddillo, G. Wells 2019. Denitrifying PAOS for low- Carbon and low-energy nutrient removal in cold weather conditions, the Ejby Mølle case study, in: 92nd Annual Water Environment Federation's Technical Exhibition and Conference, WEFTEC 2019.
- [83] S.B. Velasquez-Orta, O. Heidrich, K. Black, D. Graham, Retrofitting options for wastewater networks to achieve climate change reduction targets, *Appl. Energy* 218 (2018) 430–441, <https://doi.org/10.1016/j.apenergy.2018.02.168>.
- [84] R. Venkatramanan, O. Prakash, T. Woyke, P. Chain, L.A. Goodwin, D. Watson, S. Brooks, J.E. Kostka, S.J. Green, Genome sequences for three denitrifying bacterial strains isolated from a uranium- and nitrate-contaminated subsurface environment, *Genome Announc.* 1 (2013), <https://doi.org/10.1128/genomeA.00449-13>.
- [85] B. Wang, J. Li, L. Wang, M. Nie, J. Li, Mechanism of phosphorus removal by SBR submerged biofilm system, *Water Res.* 32 (1998) 2633–2638, [https://doi.org/10.1016/S0043-1354\(97\)00413-2](https://doi.org/10.1016/S0043-1354(97)00413-2), DOI: 10.1016/S0043-1354(97)00413-2.
- [86] R. Wang, P. Wilfert, I. Dugulan, K. Goubitz, L. Korving, G.J. Witkamp, M.C.M. van Loosdrecht, Fe(III) reduction and vivianite formation in activated sludge, *Sep. Purif. Technol.* 220 (2019) 126–135, <https://doi.org/10.1016/j.seppur.2019.03.024>.
- [88] H. Wickham, M. Averick, J. Bryan, W. Chang, L.D. McGowan, R. François, G. Grolemond, A. Hayes, L. Henry, J. Hester, M. Kuhn, T.L. Pedersen, E. Miller, S. M. Bache, K. Müller, J. Ooms, D. Robinson, D.P. Seidel, V. Spinu, K. Takahashi, D. Vaughan, C. Wilke, K. Woo, H. Yutani, Welcome to the {tidyverse}, *J. Open Source Softw.* 4 (2019) 1686, <https://doi.org/10.21105/joss.01686>.
- [89] H. Wickham, R. François, L. Henry, K. Müller, 2018. dplyr: A Grammar of Data Manipulation.
- [90] P. Wilfert, A. Mandalidis, A.I. Dugulan, K. Goubitz, L. Korving, H. Temmink, G. J. Witkamp, M.C.M. Van Loosdrecht, Vivianite as an important iron phosphate precipitate in sewage treatment plants, *Water Res.* 104 (2016) 449–460, <https://doi.org/10.1016/j.watres.2016.08.032>.
- [91] K. Yamagiwa, A. Ohkawa, O. Hirasaka, Simultaneous Organic Carbon Removal and Nitrification by Biofilm Formed on Oxygen Enrichment Membrane, *J. Chem. Eng. Japan* 27 (1994) 638–643.
- [92] S.-H. Yoo, H.-Y. Weon, B.-Y. Kim, J.-H. Kim, Y.-K. Baek, S.-W. Kwon, S.-J. Go, E. Stackebrandt, *Pseudoxanthomonas yeongjuensis* sp. nov., isolated from soil cultivated with Korean ginseng, *Int. J. Syst. Evol. Microbiol.* 57 (2007) 646–649, <https://doi.org/10.1099/ijs.0.64427-0>.